Nanoscale

REVIEW

View Article Online
View Journal | View Issue

Check for updates

Cite this: *Nanoscale*, 2025, **17**, 13145

Research progress of transition metal catalysts for electrocatalytic EG oxidation

Hongjing Wu,[a] Xiaoyue Zheng,[a] Jiajia Liu,[a] Yanru Yuan,[a] Yuquan Yang,[a] Chenjing Wang,[a] Li Zhou,[a] Lulu Wang,[a] Binbin Jia,*[b] Xiaoyu Fan*[c] and Jinlong Zheng *[a,d]

Received 28th November 2024,
Accepted 8th April 2025

DOI: 10.1039/d4nr05000b

rsc.li/nanoscale

Ethylene glycol (EG) is a small-molecule alcohol with a low oxidation potential and is a key monomer in the production of polyethylene terephthalate (PET). The efficient oxidation of EG can further enable the recycling of waste PET. Currently, there are many studies on catalysts for EG oxidation, among which transition metal catalysts (including traditional non-precious metals such as Fe, Co, Ni and other noble metals such as Pt and Pd) have good prospects for application in EG oxidation reactions due to their unique electronic structures. In this study, the synthesis strategy of transition metal catalysts for the electrocatalytic oxidation of EG is summarized and the performance of different types of catalysts in the EG oxidation reaction is reviewed. Advanced characterization methods were used to understand the oxidation mechanism of EG and to control the conversion of EGOR intermediates into target products. Therefore, we need to further explore efficient catalysts for EG oxidation to achieve efficient reactions.

Published on 12 d'abril 2025. Downloaded on 14/2/2026 0:11:27.

[a]*Beijing Advanced Innovation Center for Materials Genome Engineering, School of Mathematics and Physics, University of Science and Technology Beijing, Beijing 100083, China. E-mail: zhengjinlong@ustb.edu.cn*
[b]*College of Materials and Chemical Engineering, Key Laboratory of Inorganic Nonmetallic Crystalline and Energy Conversion Materials, China Three Gorges University, Yichang 443002, China*
[c]*Beijing Key Laboratory for Optical Materials and Photonic Devices, Department of Chemistry, Capital Normal University, Beijing 100048, China*
[d]*Shunde Innovation School, University of Science and Technology Beijing, Foshan 528399, China*

1. Introduction

With the carbon neutrality policy, people are ever more concerned about the environment, so some waste with recycling value could be processed by relevant means to achieve the upgrading of waste. The treatment of 'white pollution' has been troubling relevant researchers, so it is of far-reaching research significance to realize the recycling of plastics. Polyethylene terephthalate[1] (PET) is a kind of plastic used for

Hongjing Wu

Hongjing Wu is a Masters candidate at the School of Mathematics and Physics University of Science and Technology Beijing under the supervision of Assoc. Prof. Jinlong Zheng. Her current research interest is focused on the design and synthesis of functional nanomaterials for water electrolysis.

Jinlong Zheng

Jinlong Zheng is an associate professor in the Beijing Advanced Innovation Center for Materials Genome Engineering at the University of Science and Technology Beijing, China. He received his Ph.D. from Beihang University in the School of Chemistry in 2016. He undertook postdoctoral research at Beihang University from 2017 to 2018. His research interests focus on the synthesis of nanomaterials and nanostructures for the applications of energy-conversion devices. He is especially concerned with the development of the surface and interface engineering of advanced electrocatalysts.

Published on 12 d'abril 2025. Downloaded on 14/2/2026 0:11:27.

daily packaging and textile purposes,[2] and the apparent consumption of polyester in China has reached about 48.99 million tons by 2022. Currently, the main treatment of PET packaging waste is landfill or incineration;[3] some could be more reasonably utilized indirectly or directly, and some accumulates in the environment.[4] Such a large amount of PET consumption can still cause serious environmental pollution if it is not handled properly. Ethylene glycol (EG) is a key monomer in the production of PET. We can reduce pollution by processing hydrolyzed PET.

In the long term, it is preferable to achieve high-efficiency electrocatalytic oxidation of EG. Firstly, the polyester nature of PET leads to its easy hydrolysis under alkaline conditions, and secondly, the main monomer of PET, EG, due to the unique properties of alcohols,[5,6] is also easily oxidized (to produce formate,[7] glycolic acid[8] and other related value-added products), which can further improve the rate of hydrogen production. The use of electrochemical oxidation of PET with aqueous monomer EG has significantly reduced resource wastage and further reduced environmental pollution. For example, Zhao and colleagues made a pioneering contribution by introducing and documenting an electrochemical up-cycling method for the use of Cu-based nanowires as catalysts for the electrocatalytic oxidation of PET. In addition, electrocatalytic oxidation can directly convert chemical energy into electrical energy, avoiding the energy loss of traditional combustion methods. By selecting suitable catalysts and reaction conditions, selective control of EG oxidation products can be achieved. For example, the reaction can be regulated to produce high value-added chemicals such as formic acid, glycolic acid, glyoxylic acid, *etc*. Currently, transition metal catalysts are also a hot topic for EG oxidation. Research on the electrochemical oxidation of EG has been ongoing to date, building on the investigations of previous generations. Research on the oxidation of EG began as early as the beginning of the 20th century. Due to the relatively limited experimental techniques and analytical means available at that time, scientists only studied the basic chemical properties of EG. By the middle of the 20th century, with the continuous development of chemical analysis techniques and instruments, researchers were able to explore the mechanism of the EG oxidation reaction more deeply. The oxidation process of EG under different conditions was monitored and analyzed by means of spectroscopy, electrochemistry and other techniques, and some preliminary models of the reaction mechanism were proposed. For example, Weber presented the seminal study of the oxidation reaction of EG on the Pt electrode. This laid the foundation for subsequent related studies and allowed more researchers to start focusing on this field. At that time, the research was mainly focused on the observation of the basic phenomena of the reaction and the preliminary exploration of the reaction properties, including the conditions under which the reaction occurs, the role played by the electrode surface, and so on. However, the understanding of the reaction mechanism was still at a relatively early stage due to the technical and theoretical level at that time. Vijh made further in-depth explorations on the basis of Weber's research. He conducted a more systematic study of the oxidation reaction mechanism of EG on the Pt electrode, trying to reveal key information such as intermediates, reaction pathways, *etc*. during the reaction. The research methodology at this stage had been improved, and more advanced analytical techniques and experimental means were adopted to monitor the changes in the reaction process more accurately. Vijh's[9] research results made an important contribution to the construction of the theoretical system of the oxidation reaction of EG, and pushed the research in this field to a deeper level. From 1966 to 1971, research on the oxidation reaction of EG on the Pt electrode gradually developed from the initial starting stage to a more in-depth exploration stage, which laid an important foundation for subsequent research in this field, and provided theoretical support for the practical application of the oxidation reaction of EG. At the same time, researchers began to pay attention to the effect of catalysts on the oxidation reaction of EG, including some transition metal catalysts that were found to be able to accelerate the oxidation reaction of EG, which laid the foundation for the subsequent catalyst research. After the 21st century, that is, in the period of rapid development of catalysts for the oxidation of EG electrocatalytic oxidation, researchers have continuously explored new catalysts in order to improve EG oxidation reaction efficiency and selectivity. For example, Professor Lei Wang and Associate Professor Xu published a paper on Rh-modified $PtRh_{0.02}$@Rh[10] nanowire electrocatalysts for efficient catalysis of EG-assisted hydrogen production from seawater electrolysis, and the team of researcher Yong Chen designed and synthesized a Pd–$Ni(OH)_2$ composite electrocatalyst for the highly selective oxidation of EG. These catalysts enhanced the adsorption capacity of EG and the activation of reaction intermediates by modulating the electronic structure and generating strain effects, thus improving the activity and selectivity of the reaction. The continuous exploration of the electrocatalytic oxidation of EG has also gained wide attention in the field of electrocatalytic plastic up-cycling. The oxidation reaction of EG, as a hydrolysis product of petroleum-based PET, can convert under-utilized carbon resources into high-value-added chemicals, which provides a new way of thinking in solving the problem of white pollution and realizing the recycling of resources.

At present, research on transition metal catalysts mainly focuses on heterogeneous structure catalysts and multicomponent alloy catalysts. For example, Pd-PdSe[11] nanosheet catalysts were prepared with a unique two-dimensional heterostructure. Pd–Se compounds with low crystallinity inside the catalyst interacted with metallic Pt at the edges to produce strong d–p orbital hybridisation. The electronic structure of the catalysts was deeply modified to exhibit excellent EG oxidation performance and high C1 path selectivity in alkaline media,[8,12,13] which can more effectively promote the complete oxidation of EG. The synergistic effect between different metals can improve the electronic structure and surface properties of the catalyst, enhance the adsorption and activation

 This journal is © The Royal Society of Chemistry 2025

Published on 12 d'abril 2025. Downloaded on 14/2/2026 0:11:27.

ability of EG, and improve the catalytic activity and selectivity. For example, Ni–cobalt–manganese ternary oxide catalysts show excellent performance in the electrocatalytic oxidation of EG, with high catalytic activity and stability. Therefore, it is particularly important to select an efficient catalyst for the electrocatalytic oxidation of EG. Studies have shown that transition metal electrocatalysts have a good application prospect in the EG oxidation reaction, and the transition metal catalysts reviewed in this work are not only limited to the conventional Fe, Co, Ni-based catalysts,[14] but also include Pt, Pd, Ir[15–20] and other noble metal catalysts. These transition metal catalysts have obvious advantages in the reaction process, which are mainly manifested in the following aspects: high catalytic activity; transition metals have a variety of variable oxidation states and electronic configurations[21–23] which enable them to form specific chemical bonds with EG molecules and reaction intermediates, so as to effectively promote the oxidation reaction. For example, by changing the electronic structure of the transition metal, this can tweak its adsorption capacity for EG and the reaction active site, improving the catalytic efficiency. In some transition metal catalysts, there is a synergistic effect between different metals. For example, in binary or multicomponent transition metal alloy catalysts, the interaction between different metal atoms can change the electronic structure and surface properties of the catalyst, enhance the adsorption and activation ability of EG, and thus improve the catalytic activity. In the electrocatalytic oxidation of EG, the unique electronic structure[24] of the catalyst is the key factor improving the catalytic activity. Its effects can be summarized in three aspects: (1) orbital hybridization forms new chemical bonds and active sites, which enables the atoms in the catalyst to form new chemical bonds and produce special electron distribution. These newly formed chemical bonds and the unique electron distribution can be used as active sites to enhance the adsorption capacity of EG molecules and reaction intermediates, so as to optimize the reaction path and reduce the reaction energy barrier. (2) Due to electronegativity differences, electron transfer occurs in different elements, changing the electronic state of the metal, shifting the center of the d band, and regulating the adsorption and desorption of the reactive species, and the resulting local charge distribution affects the adsorption and desorption process of the reactive species, promoting the reaction and avoiding side reactions. (3) Defects[25] and interface structures in the catalyst cause the atomic coordination to be unsaturated, resulting in more active sites, promoting electron transport and interaction between different components and synergistic enhancement of catalytic performance. Selective control of EG oxidation products can be achieved by judicious design of the structure and composition of transition metal catalysts. For example, the complete oxidation of EG to carbon dioxide and water can be promoted to achieve higher energy conversion efficiency; or glycolic acid, glyoxylic acid and other high-value chemicals can be selectively produced to provide more options for chemical production. For example, Duan's[8] research group used an electrocatalytic oxidation strategy to oxidize ethylene glycol to a more valuable product-formamide.

Compared with transition metal precious metal catalysts (such as Pt, *etc.*), transition metal non-precious metal catalysts[26,27] (such as Ni, Co, Cu, *etc.*) have more abundant reserves on Earth and relatively low prices, so non-precious transition metal catalysts have obvious cost advantages in large-scale applications, but their performance is slightly inferior to that of precious metal catalysts. In order to develop more efficient electrocatalytic oxidation catalysts, appropriate modulation strategies can be chosen to regulate the electronic structure of the catalysts so as to improve the catalytic activity of the catalysts and further promote the marketing of the glycol electrocatalytic oxidation technology.

The catalytic activity, selectivity and stability of transition metal electrocatalysts for EG oxidation can be improved by designing and controlling the structure, composition and electronic properties of transition metal electrocatalysts. However, transition metal electrocatalysts still face many challenges in EG oxidation, such as the catalytic activity needs to be further improved, the stability and durability are insufficient, and the cost is high. It is of great importance to study the mechanism of the transition metal electrocatalyst in EG oxidation and develop a new and efficient catalyst system to promote the practical application of direct alcohol fuel cells. Based on this, firstly, the oxidation mechanism of EG under alkaline condition is described in this work. Secondly, the synthesis methods and catalytic performance of the electrocatalysts used for glycol oxidation are described, and some problems existing in the current catalysts are described, which provide reference significance for the further exploration of high-performance electrocatalytic oxidation of glycol transition metal catalysts.

2. EGOR reaction mechanism of transition metal catalysts

The essence of EG oxidation is that, under certain conditions, the C–H bond or carbon–carbon bond in the EG molecule breaks, reacts with the oxidising agent and loses electrons so that it is oxidised. During the oxidation process, functional groups such as hydroxyl (–OH) in glycol molecules can participate in the reaction, resulting in changes in its structure and the formation of various oxidation products. For the oxidation reaction of EG the earliest research was about its normal oxidation reaction,[28] but with the continuous exploration of researchers, research on the electrocatalytic oxidation reaction of EG has developed rapidly, and nowadays the literature is mostly about the electrocatalytic oxidation of EG. However, this does not mean that there is no difference between these two reactions. For the oxidation of EG,[29] an oxidant is usually required, such as potassium permanganate, oxygen, *etc.*, and there are certain requirements for the reaction temperature, pressure and other conditions. The conditions for such oxidation reactions are relatively harsh, requiring a specific chemical environment and a high energy input. In contrast, electrochemical studies have traditionally focused more on the potential–current behavior on different catalysts as well as the

Published on 12 d'abril 2025. Downloaded on 14/2/2026 0:11:27.

oxidation products. The electrocatalytic oxidation reaction of EG, which is usually carried out in an electrochemical system, requires conditions such as electrodes, electrolytes, and an applied electric field.

The oxidation of EG occurs on the electrode surface by applying a voltage across the electrode. The reaction conditions are relatively mild and can be carried out at room temperature and pressure, and the rate and selectivity of the reaction can be controlled by adjusting parameters such as voltage and current. There is also a certain difference between the two in the mechanism of the reaction. In the oxidation of EG reaction process, the oxidant directly chemically reacts with EG, through the capture of glycol molecules in the electron or hydrogen atom to achieve oxidation. During the reaction, the nature of the oxidant and the reaction environment have an important influence on the type and distribution of the oxidation products. In the electrochemical oxidation of EG process, the EG molecule is firstly adsorbed on the surface of the electrode, and then under the action of the electric field the active sites on the surface of the electrode interact with the EG, so that the EG loses its electrons and undergoes the oxidation reaction. At the same time, the ions in the electrolyte will also participate in the reaction, playing the role of transferring charge and maintaining electroneutrality. In general, the electrochemical oxidation of EG has a higher reaction rate and higher selectivity, so the study of electrochemical oxidation of EG is more relevant. The oxidation reactions of EG mentioned in this paper are electrochemical oxidation of EG.

In general, glycol oxidation is a chemical reaction process involving the breaking of chemical bonds and electron transfer. The reaction follows different reaction mechanisms in different media. The pathway of electrocatalytic oxidation of EG in alkaline medium is generally divided into two cases: a complete oxidation with multi-step dehydrogenation,[30] where the EG molecule ($HOCH_2CH_2OH$) undergoes adsorption on the electrode surface with the aid of the catalyst. Immediately thereafter, in an alkaline environment, the α-H of the EG molecule is affected by the neighboring hydroxyl group and its activity is enhanced, and it is easily adsorbed by the active site on the catalyst surface and α-H removed. At the same time, it combines with OH^- in solution to produce the intermediate in adsorbed state ($HOCH_2CH(OH)O^*$), which releases an electron, which is the first step of the reaction for dehydrogenation. Subsequently, the intermediate is further dehydrogenated, and after a multi-step reaction, the carbon–carbon bond is broken. After the break, the hydroxyl group on one of the carbon atoms continues to dehydrogenate and reacts with OH^- to formate ($HCOO^-$); the other carbon atom undergoes a similar process of dehydrogenation and combination with OH^- to produce formate, which also continues to dehydrogenate and oxidize gradually to carbonate. In addition to the complete oxidation path, there is also a partial oxidation path in which the carbon–carbon bond is not broken.[17] EG is first dehydrogenated to produce glyoxal (OHC-CHO), which continues to react with OH^-, undergoes further oxidation and addition reactions, and ultimately produces products such as glycolate ($HOCH_2COO^-$) and oxalate. A variety of intermediates are generated during the reaction process; in addition to the intermediates in the adsorbed state ($HOCH_2CH(OH)O^*$) and glyoxal mentioned earlier, there are also ethanol aldehydes ($HOCH_2CHO$), ethanoic acid ($HOCH_2COOH$), and glycolic acid (OHCCOOH), *etc*., which are generated at different stages of the reaction and can be transformed with each other through a series of redox reactions. In the electrocatalytic oxidation of EG in alkaline medium, the breaking of the carbon–carbon bond is the decisive step of the whole reaction. Due to the large bond energy of the carbon–carbon bond, its breaking needs to overcome a high energy barrier,[31] so it is relatively slow kinetically. At the same time, the type and nature of the catalyst have an important influence on the rate of carbon–carbon bond breaking. Some catalysts with special crystal structures and active sites can effectively reduce the activation energy of carbon–carbon bond breaking and thus accelerate the reaction rate. In acidic media, the concentration of protons (H^+) is higher in the reaction system, which is significantly different from the reaction mechanism in alkaline media. After adsorption on the electrode surface, the EG molecule first undergoes dissociative adsorption in which the hydrogen atom on one of the hydroxyl groups detaches to form an intermediate in the adsorbed state ($HOCH_2CH_2O^*$) and releases a proton and an electron. Subsequently, the intermediate undergoes further dehydrogenation to produce glyoxal. Glyoxal continues to react with water in an acidic environment and undergoes a series of oxidation and dehydration processes to produce glycolic acid ($HOCH_2COOH$). Glycolic acid can also continue to oxidize, gradually removing hydrogen atoms and eventually producing carbon dioxide (CO_2). This is a more complex multi-step reaction process involving the transfer of multiple electrons and protons. The main components of the reaction process include intermediates in the adsorbed state ($HOCH_2CH_2O^*$), glyoxal, glycolic acid, oxalic acid (HOOC-COOH), and carbon monoxide (CO). Among them, carbon monoxide is a very critical intermediate product, which has strong adsorption capacity and is easily adsorbed on the active sites on the catalyst surface to form strongly adsorbed CO_{ads} species,[32] leading to the poisoning of the catalyst and thus inhibiting the further progress of the reaction. In addition, oxalic acid is also an important intermediate product in the reaction process, which can be generated by further oxidation of ethanoic acid and can also under certain conditions undergo a decomposition reaction to generate carbon dioxide and other products. There exist several views on the decisive speed step in acidic media. One view is that the adsorption and desorption of carbon monoxide on the catalyst surface is the decisive step. Since carbon monoxide binds strongly to the active sites on the catalyst surface, its desorption needs to overcome a high energy barrier, so if carbon monoxide cannot be desorbed from the catalyst surface in time, it will occupy the active sites and hinder the subsequent reaction. Another view is that the further oxidation of ethanoic acid is a decisive step because it involves the breaking and formation of several chemical bonds and the reaction kinetics are relatively slow.

 This journal is © The Royal Society of Chemistry 2025

Published on 12 d'abril 2025. Downloaded on 14/2/2026 0:11:27.

It is the fact that the electrocatalytic oxidation of EG has different reaction mechanisms in different media that also places requirements on the choice of catalyst. For example, the electrochemical oxidation of EG achieved on cobalt, Ni and iron electrodes cannot be carried out under acidic conditions, whereas precious metals are able to achieve the electrochemical oxidation of EG in both acidic and alkaline media. For non-precious metal Fe, Co and Ni electrodes, acidic processes react and the adsorption process is blocked. Under acidic conditions, EG molecules need to be adsorbed to the active sites on the electrode surface for subsequent oxidation reactions. However, the surfaces of cobalt, Ni, and iron electrodes tend to form oxide or hydroxide layers in acidic environments. These surface layers change the properties of the electrode surface, making it difficult for glycol molecules to be adsorbed effectively. For example, iron electrode surfaces may form a precipitated layer of iron hydroxide ($Fe(OH)_3$) in acidic solutions, preventing glycol molecules from coming into contact with active sites on the electrode surface, making it difficult for the glycol molecules to interact strongly enough with the covered active sites to initiate an oxidation reaction. Not only that, these metals (cobalt, Ni, and iron) have low electrode potentials in acidic environments and are susceptible to oxidation reactions, causing a change in the electron cloud density on the metal surface. This change causes the active sites on the metal surface (usually unsaturated coordination sites of some metal atoms) to be occupied by anions or water molecules in solution. The intermediates produced by the oxidation of EG are unstable under acidic conditions. In the case of aldehyde intermediates generated by EG oxidation, for example, under acidic conditions the aldehydes may undergo further side-reactions with hydrogen ions in solution, rather than following the desired oxidation pathway to carboxylic acids and other end products. In the case of precious metals, the above problems can be effectively avoided due to their stable nature. They effectively adsorb glycol molecules in both acidic and basic media. This is due to the fact that precious metals have suitable atomic spacing and electronic structure, and their surface atoms are able to form chemical bonds or stronger adsorption with functional groups[33] in the EG molecule. For example, the atoms on the surface of the Pt electrode can combine with the hydroxyl group of the EG molecule through coordination bonding and other ways to fix the EG molecule on the surface of the electrode, and this adsorption can make the chemical bond of the EG molecule undergo a certain degree of polarization, reduce the activation energy required for the reaction, and create favorable conditions for subsequent oxidation reactions. The redox potential of the precious metal electrode is relatively stable in acidic and alkaline media, and will not be easily hindered by the media like Co, Ni and Fe electrodes. Under acidic conditions, the noble metal electrode can provide a suitable electronic energy state, so that the electrons in the alcohol[34] molecule can be smoothly transferred to the electrode, promoting the oxidation reaction. Under alkaline conditions, although the solution environment changes, the noble metal electrode can likewise maintain a stable electron transfer channel with the EG molecule by adjusting the electronic state on its surface. For example, in alkaline solution, the noble metal electrode can establish an effective electron transfer path with the EG anion to ensure that the oxidation reaction proceeds in an orderly manner. During the oxidation of EG, the noble metal electrode can also effectively guide the reaction intermediates to follow the expected oxidation path. Thus, the surface properties of the precious metal electrode stabilize the reaction intermediates in both acidic and alkaline media. The different breaking of the C–C bond of EG during the reaction process leads to the emergence of different oxidation pathways, which can be classified as the C1 pathway and C2 pathway according to the difference in the products of electrocatalytic oxidation. The C1 pathway is a complete oxidation pathway, which indicates that EG is completely oxidized. The single carbon products of the electrocatalytic oxidation of EG include carbon dioxide and formic acid. When oxidized to CO_2, the carbon–hydrogen and carbon–carbon bonds in the molecule of EG in the electrocatalytic process are progressively broken by oxidation, and after a series of intermediate reaction steps, eventually all carbon atoms are completely oxidized and converted into products such as carbonates, and this process involves more electron transfer processes, which can release a total of 10 electrons. Fig. 1a shows two common oxidation products of EG oxidation. Different catalytic electrodes can result in different adsorbed species in the centre, leading to different cleavage positions of the C–C bonds to form different EG oxidation derivatives. In this process of electrocatalytic oxidation of EG achieved by Ni and Co electrodes as anode electrodes in the figure, the oxidation product of the C1 oxidation pathway is formic acid, and the whole process involves 6 electrons in the reaction. As for the C2 pathway, the figure shows that the carbon–carbon bond of the EG molecule is partially broken, not completely disconnected, and part of the carbon chain structure is retained. This process involves 4 electron transfers in the whole reaction process, and its oxidation product is usually the generation of glycolate. During the reaction process EG is first adsorbed on the electrode surface, then the hydroxyl group is oxidized to form intermediate products such as ethanol aldehyde, which is further oxidized to produce ethanoate and oxalate *etc*. For this process, a lower degree of oxidation is required, which is more likely to occur under some specific catalysts and reaction conditions, but the selectivity of its oxidation products is lower. One of the C2 products, namely glycolic acid,[35] has a high application value in the chemical field and can be used as a raw material for the synthesis of other organic compounds, so the efficient oxidation of EG to glycolic acid can be focused on in the subsequent investigation process. Ma *et al.*[36] studied the influence of different catalysts on carbon–carbon bond cleavage using *in situ* infrared and Raman spectroscopy, and used *in situ* infrared absorption spectroscopy for real-time detection to illustrate the products and intermediates in the reaction process. On this basis, the EGOR catalytic activity of Co and Ni electrodes was further understood. Fig. 1b shows *in situ* infra-

Published on 12 d'abril 2025. Downloaded on 14/2/2026 0:11:27.

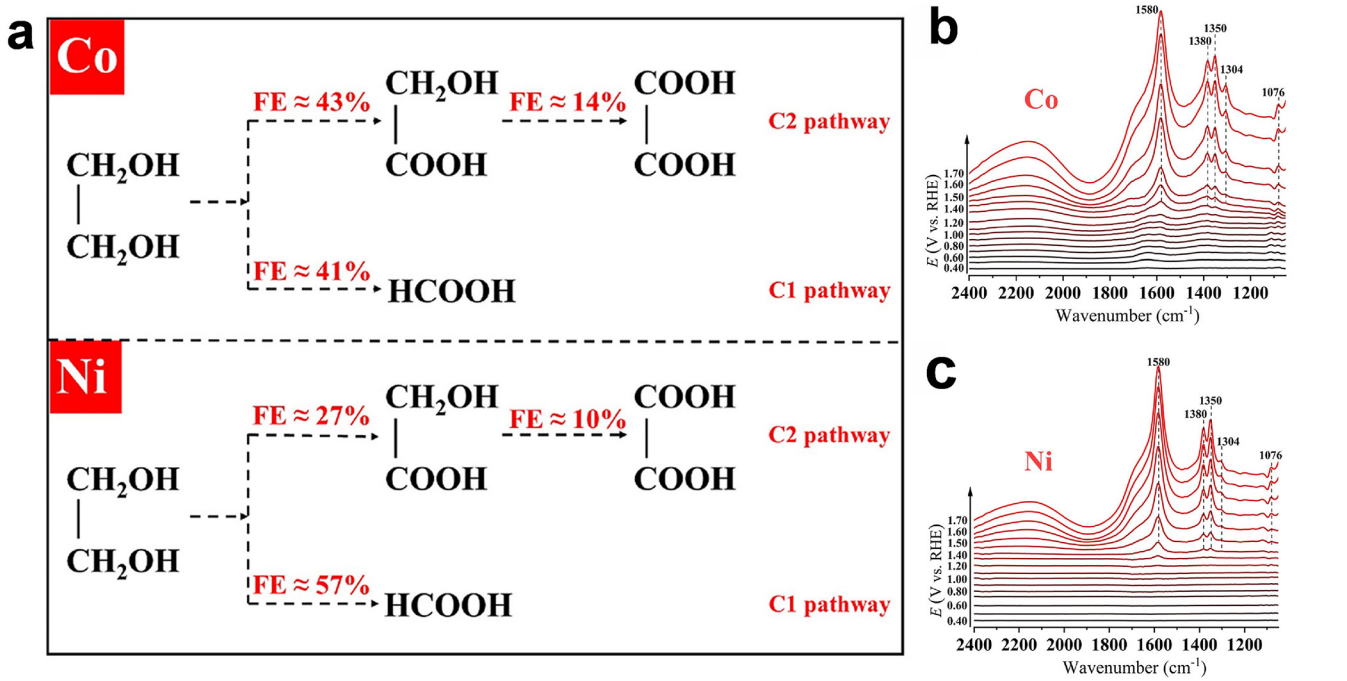

Fig. 1 (a) Oxidation pathway diagram of EG at Ni and Co electrodes, *in situ* IRAS spectra recorded at (b) Co and (c) Ni electrodes in 1 M NaOH with 1 M EG, reproduced with permission.[36] Copyright 2023, Elsevier.

red spectra of Ni and Co electrodes in alkaline electrolyte at different potentials ranging from 0.40 to 1.70 V. Among them, 1580, 1380 and 1350 cm^{-1} can be considered as the asymmetric stretching vibration of O–C–O formate.

The simultaneous detection of signals in the 1580, 1350 and 1076 cm^{-1} bands indicates the presence of glycolic acid, and the vibration signals in the 1580 and 1304 cm^{-1} bands are considered to be the characteristic peak emergence response of oxalates. Therefore, based on the *in situ* infrared test results, it is concluded that the oxidation reaction of EG on the surface of Co and Ni can produce formates, glycolates and oxalates. However, on the surface of the Co electrode, the band intensity of the 1076 cm^{-1} band is significantly higher, indicating that EG is more easily oxidised to glycolic acid on the surface of the Co electrode than the Ni electrode, and the most probable oxidation path of different catalysts is further inferred. Therefore, the oxidation of EG will more easily obtain the target product by reasonable regulation of the catalyst.

3. Synthesis method of transition metal catalyst

3.1 Hydrothermal/solvothermal synthesis strategies

The hydrothermal method is a widely used catalyst synthesis method, which can precisely control the structure, morphology and electronic state of electrocatalysts, and is helpful in the synthesis of materials with a high number of catalytic active sites. In addition, by the judicious design of reaction conditions and selection of suitable precursors, electrocatalysts with unique structures,[37] such as nanostructures[38] and porous structures,[39] can be prepared, which can provide more active sites and increase the contact area between the reactants and the catalyst, thereby improving the efficiency of the catalytic reaction. For example, electrocatalysts with morphologies such as nanowires and nanosheets[40] synthesised by hydrothermal methods show excellent catalytic activity in electrocatalytic processes such as the hydrogen evolution reaction,[31] oxygen evolution reaction[13,41] and other organic oxidation reactions. In addition, the preparation method can precisely regulate the morphology[42] of the electrocatalyst by changing the temperature, pressure, reaction time, reactant concentration and other conditions during the synthesis process.[43] Different morphologies also have different specific surface areas, numbers of exposed active sites and electron transport properties, and thus can meet the needs of different electrocatalytic reactions. On the other hand, in the hydrothermal reaction system, it is easy to introduce other elements or compounds for doping and modification of the electrocatalysts, so as to improve the activity of the catalysts. At present, this preparation method is commonly used for electrocatalysts for EG oxidation. For example, Qian *et al.*[33] synthesized a NiVRu-LDHs NAs/NF electrode by a simple one-step hydrothermal method. The detailed synthesis process is shown in Fig. 2a. $Ni(NO_3)_2$-$6H_2O$, VCl_3 and urea were dissolved in 30 mL of deionised water, and then $RuCl_3$ aqueous solution was added to finally obtain the mixed solution at 120 °C for 12 hours of hydrothermal reaction to obtain the NiVRu-LDHs electrode material grown on Ni foam. Qiao *et al.* also used a simple hydrothermal synthesis method to convert CuO into RhCu nano capsules. As shown in Fig. 2b,

 This journal is © The Royal Society of Chemistry 2025

Published on 12 d'abril 2025. Downloaded on 14/2/2026 0:11:27.

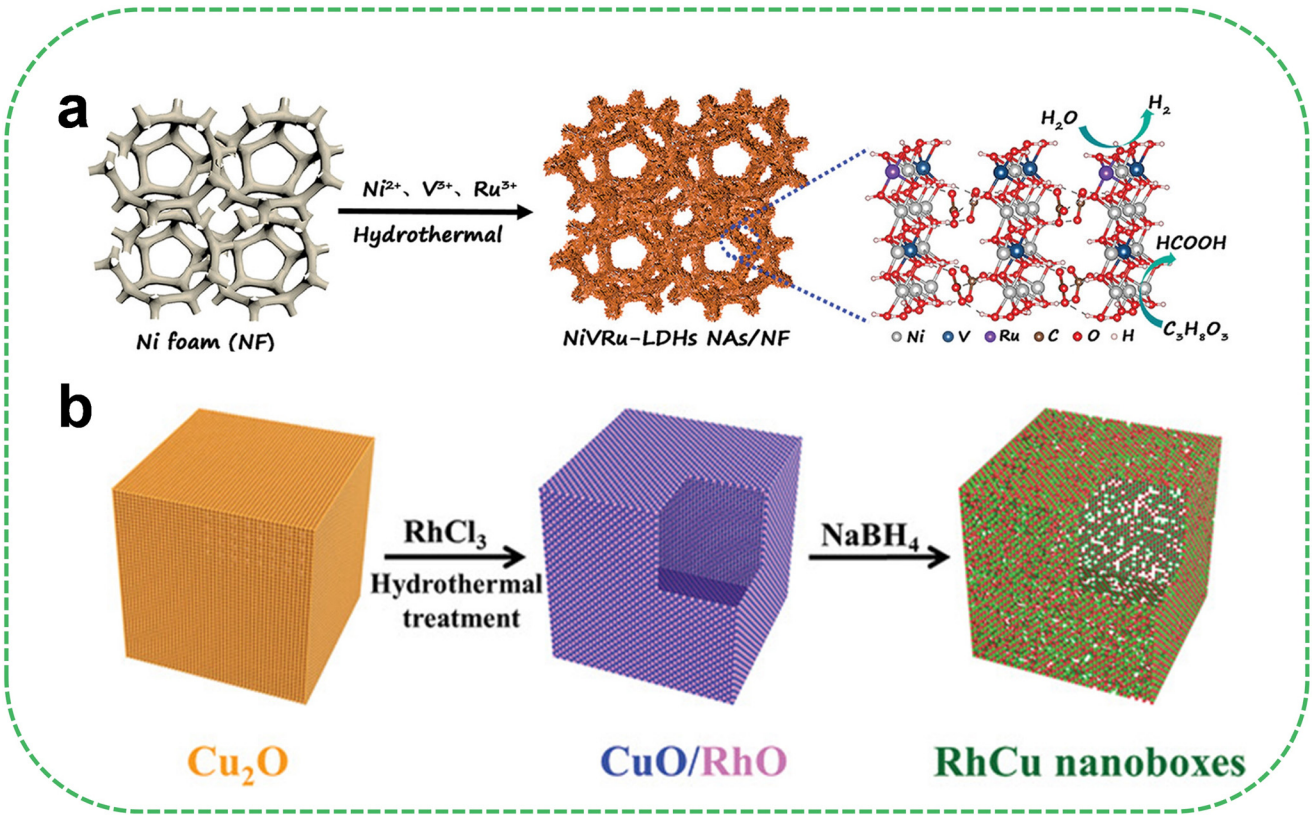

Fig. 2 (a) Preparation flowchart of NiVRu-LDHs NAs/NFs, reproduced with permission.[33] Copyright 2023, John Wiley and Sons. (b) Preparation flowchart of RhCu nanomaterial, reproduced with permission.[16] Copyright 2021, John Wiley and Sons.

2 mL of $RuCl_2$ solution was added to the Cu_2O nano cube suspension.[16] The mixture was then reacted at 150 °C for 6 hours in a Teflon-lined stainless-steel autoclave. After cooling, the solid products were collected by centrifugation and washing with deionised water, and finally the RhCu nano cellular electrode material was obtained.

3.2 Wet chemical synthesis strategy

Wet chemical synthesis of electrocatalysts is also an important method of preparation, entailing the conversion of reactants into target electrocatalysts through chemical reactions in a solution system. The core principle is to control the reaction conditions by using the interactions and chemical reactions of ions and molecules in the solution to regulate the composition, structure and performance of the electrocatalysts; *e.g.*, by controlling parameters such as the reaction temperature, concentration, and pH, the reaction rate, product morphology, and degree of crystallinity can be affected. In the actual synthesis process, appropriate metal salts, metal oxides, organic compounds, *etc*. can be selected as the reactants according to the composition and structure of the target electrocatalysts, and the specific ratio can be determined. These reactants usually need to be dissolved in suitable solvents to form a homogeneous reaction solution by heating and other methods. As shown in Fig. 3a, Wang *et al.*[44] successfully prepared Pd/A-MnO_2 by a two-step wet chemical strategy, reduced $KMnO_4$ into amorphous MnO_2 using NaH_2PO_2 as a reducing agent, and further introduced ultrafine Pd nanoparticles onto amorphous MnO_2 nanosheets by a hydrothermal method. The abundant defects on the surface of the amorphous MnO_2 nanosheets increased the loading amount of Pd nanoparticles, enhanced the formation of Pd nanoparticles and further improved the catalytic activity of the electrodes. Li *et al.*[45] chose the types and proportions of solvents and surfactants as variables to prepare a series of Ni selenide samples with different morphologies, which further proved that the structure can be regulated by wet chemistry. As shown in Fig. 3b, Ni $(acac)_2$, Se powder and OAM were dissolved in a DDT vial and the resulting solution was then reacted with appropriate amounts of OAM, ODE and OA in a three-necked flask at 230 °C for 20 minutes to obtain the final sample. Different OAM/ODE/OA ratios were adjusted to obtain $NiSe_2$ with different geometries.

3.3 Electrochemical synthesis strategy

Electrochemical synthesis methods mainly include the electrodeposition method, anodic oxidation method, cathode reduction method, electrochemical etching method, *etc*., with different focuses. For example, the electrodeposition method uses an electrolyte containing metal ions and the application of an external electric field, so that metal ions on the surface of the electrode undergo a reduction reaction and deposition

Published on 12 d'abril 2025. Downloaded on 14/2/2026 0:11:27.

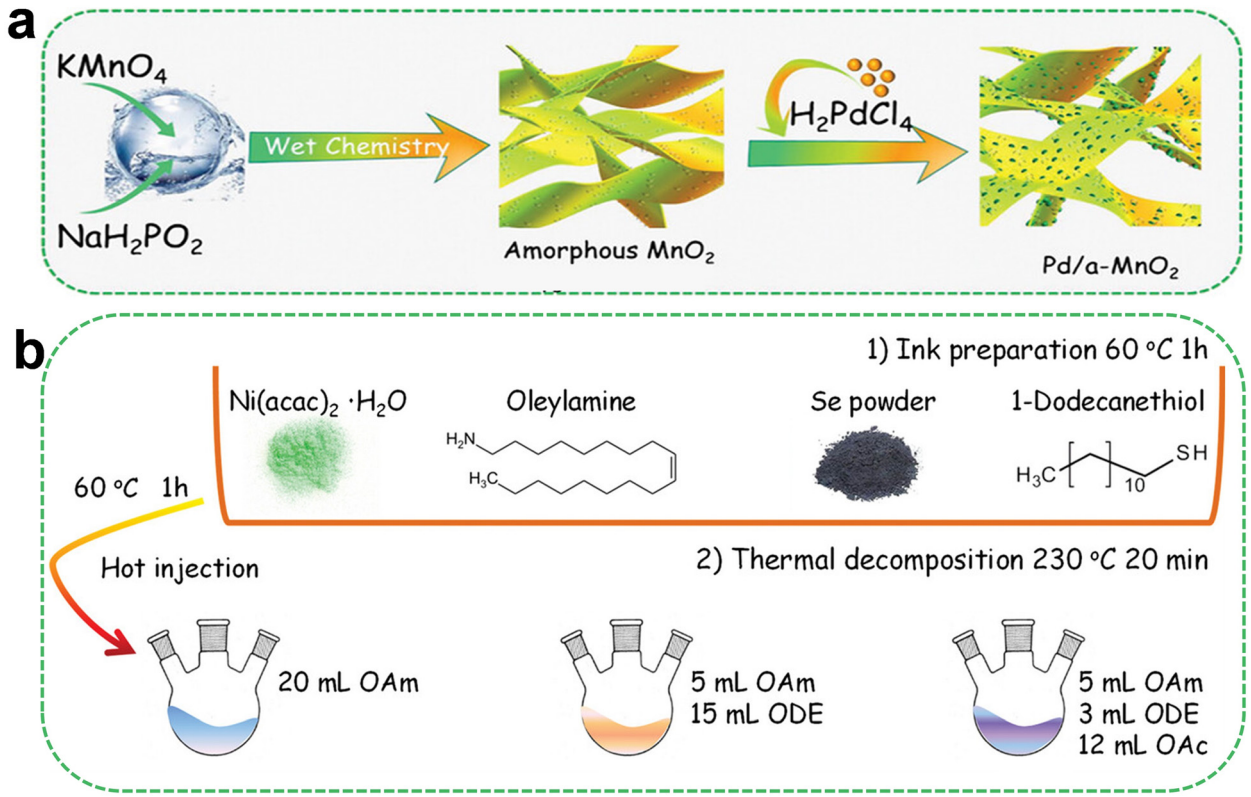

Fig. 3 (a) Preparation flow chart of Pd/A-MnO_2, reproduced with permission.[44] Copyright 2023, John Wiley and Sons. (b) Composite diagram of $NiSe_2$, reproduced with permission.[45] Copyright 2023, John Wiley and Sons.

to form a catalyst; for the synthesis of a glycol oxidation catalyst, a suitable metal salt solution, such as cobalt salt, Ni salt, *etc*., can be selected to be electrodeposited on a specific electrode to form a specific catalyst. During the synthesis process, the loading, morphology and structure of the catalyst can be regulated by controlling the deposition time, potential or current. For example, by changing the time of electrodeposition, the coverage of the catalyst on the electrode surface can be controlled, by changing the potential, the crystallinity and particle size of the catalyst can be influenced, *etc*. Electrodeposition is also the electrochemical synthesis method that we mainly discuss. Duan *et al.* chose the electrochemical product method to load Au atoms onto the substrate. For example, as shown in Fig. 4a, Kang *et al.*[46] also deposited Cu on NiCu/NF electrodes by cathodic electrodeposition,

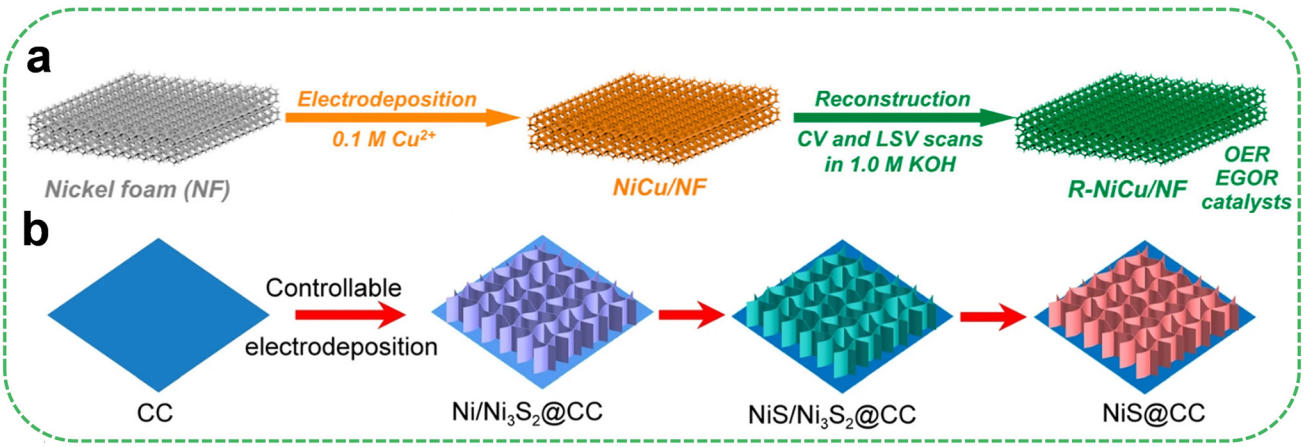

Fig. 4 (a) Flowchart of preparation of NiCu/NF, reproduced with permission.[46] Copyright 2024, American Chemical Society. (b) Composite view of NiS@CC, reproduced with permission.[47] Copyright 2024, Springer Nature.

This journal is © The Royal Society of Chemistry 2025

Published on 12 d'abril 2025. Downloaded on 14/2/2026 0:11:27.

and the electrode with the best performance was obtained with a suitable deposition time. Then, the active EGOR catalyst was formed after a reconstruction process (R-NiCu/NF), and was scanned by cyclic voltammetry (CV) and linear sweep voltammetry (LSV). As shown in Fig. 4b, Li *et al.*[47] prepared a series of Ni sulfidic-based heterogeneous interfaces at different potentials by electrodeposition. The electrodes prepared by this method also showed excellent catalytic performance in the EGOR.

3.4 Pyrolytic synthesis strategy

Electrocatalysts with high activity can be synthesized through in-depth study of the pyrolysis mechanism of the target catalysts, selection of suitable precursors and optimization of the pyrolysis conditions. In the pyrolysis strategy, high temperature can promote the reduction and crystallization of metal ions to form metal nanoparticles with specific structures. Fig. 5a shows that Wang *et al.*[48] further modified the catalytic material by pyrolysis based on the synthesis of Ni(II)/MSC-ZIF-67. First, Ni(II)/MSC-ZIF-67 electrode material was synthesised by wet chemistry, and then Ni(II)/MSC-ZIF-67 was heated in air at a heating rate of 5 °C min^{-1} at 350 °C for 1 h to obtain OMSNi1-Co_3O_4. NaH_2PO_2 and OMS-Ni1-Co_3O_4 were placed in the upstream and downstream of the porcelain boat, respectively, and then heated at 300 °C for 1 h to finally obtain the phosphating catalytic electrode OMS-Ni1-CoP. The results showed that phosphide has a good application prospect as a catalyst for EG oxidation. As shown in Fig. 5b, Zhang *et al.*[49] undertook further phosphidation of the CoNi-LDH electrode material by the pyrolysis method, and finally obtained the Co_2P–Ni_2P/CC catalyst by reacting in a tube furnace for 4 minutes. The $CoNi_{0.25}(OH)_2$/NF prepared by the Zhou[7] team also had excellent EG oxidation performance. Based on the synthesis of $CoNi_{0.25}(OH)_2$/NF, NaH_2PO_2 was used as the phosphorus source, and the final catalyst was obtained by phosphating at 300 °C for 2 hours in a tube furnace. Different synthesis strategies affect the microstructure of electrocatalyst to some extent. A comparison of the different synthesis strategies is shown in Table 1. The different microstructure of the catalyst will also affect the performance of the electrocatalytic oxidation of EG, including crystal structure, surface morphology, particle size, alloying and doping, interface structure and so on. In the crystal structure, the change of lattice parameters, such as the expansion or contraction caused by alloy formation, and different crystal phase states, will affect the exposure of active sites and electron transport, optimize the adsorption energy of intermediate products, and improve the catalytic performance. In terms of surface morphology, high specific surface area can provide more reaction sites, roughness increases the contact area and promotes the transport of reactants, and surface defects as active sites reduce the activation energy of the reaction. In terms of particle size, nano-sized particles have the advantages of a high number of active sites and short transport distance, and uniform size distribution ensures consistent catalytic activity. The synergistic effect of alloying and doping and the regulation of electronic structure can optimize the adsorption energy of intermediates and accelerate the reaction process through the effects of strain ligand and dual functionality. In the interfacial structure, a good metal–carrier interfacial interaction enhances the stability and electron transport, and the special environment of the heterostructure interface promotes the adsorption and activation of reactants. In the following discussion, the relationship between the electronic structure of the catalyst and electrocatalytic EG is discussed.

4. Application of transition metal catalysts in EGOR

4.1 Non-precious metal catalyst

The application of transition metal catalysts in the electrocatalysis of EG has a good application prospect,[50] the reserves of non-noble metals (such as Ni, cobalt, manganese, *etc.*) are relatively abundant in nature, and the acquisition and processing costs are low. Therefore, non-precious metal electrocatalysts have obvious economic advantages in large-scale applications,

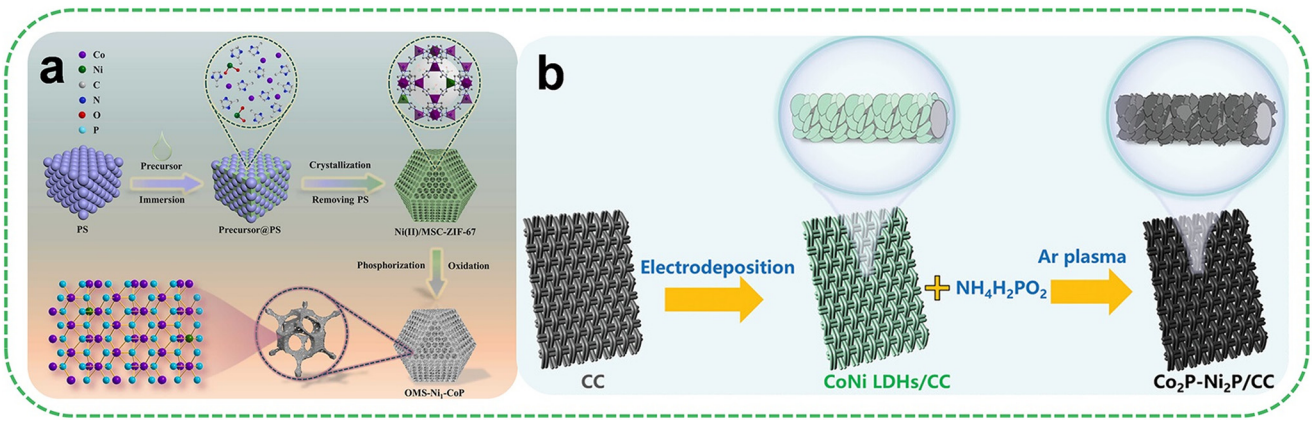

Fig. 5 (a) Preparation flow chart of Ni(II)/MSC-ZIF-67, reproduced with permission.[48] Copyright 2022, Elsevier. (b) Composite diagram of Co_2P–Ni_2P/CC, reproduced with permission.[49] Copyright 2024, John Wiley and Sons.

Published on 12 d'abril 2025. Downloaded on 14/2/2026 0:11:27.

Table 1 Comparison between different synthetic strategies used as catalysts for electrochemical oxidation of EG

Synthesis strategies	Principle	Reaction equipment	Applicable material	Advantages	Limitations
Hydrothermal/solvothermal synthesis strategies	Hydrothermal synthesis method refers to the method of synthesis by chemical reaction of substances in aqueous solution under closed conditions.	Hydrothermal synthesis reactor	Metal oxides, hydroxides, *etc.*	1. Directly prepare good crystalline powder. 2. Avoid volatilization and pollution of the reactants. 3. The shape and size of the product can be controlled.	1. The pressure resistance of the reaction equipment is high. 2. The reaction process requires high temperature and pressure.
Wet chemical synthesis strategy	The catalyst was synthesized by the interaction and chemical reaction of ions and molecules in the solution.	Oil bath pots, water bath pots and other equipment	Metal nanomaterials, metal oxides, metal hydroxides, alloys, *etc.*	1. Morphology and size of the product can be accurately controlled. 2. Reaction conditions are relatively mild. 3. Suitable for mass synthesis of two-dimensional metal nanomaterials and other electrocatalysts.	1. The reaction process may need to use a large number of solvents and chemical reagents, and the subsequent separation and purification process is more complicated. 2. The control requirements for reaction conditions are high.
Electrochemical synthesis strategy	The principle of electrochemical synthesis revolves around REDOX reaction, ion migration and Nernst equation.	Electrochemical reaction system: electrolytic cell electrode; electrochemical-workstation	Metal nanocrystals, metal elements or alloys	1. The morphology, size and structure of the catalyst can be precisely controlled. 2. Synthesis process is carried out at normal temperature and pressure.	1. The synthesis speed is relatively slow. 2. The selection and treatment of electrolyte requires certain technology.
Pyrolytic synthesis strategy	The key method of preparing high-performance electrocatalyst is to precisely control each link of pyrolysis process.	Tubular furnace; quartz boat ceramic crucible	Carbon-based materials, metal–carbon composite materials, metal phosphide, *etc.*	1. Can achieve heteroatom doping. 2. Relatively simple, easy to operate.	1. The pyrolysis process requires precise control of temperature, time and other parameters. 2. Some by-products or impurities may be produced.

which can reduce the cost of catalysts in the oxidation process of EG, and are of great significance to improve the economic benefits of related industries. In addition, catalysts with high catalytic activity can be obtained by appropriate design and control. For example, by controlling the crystalline phase, morphology and size of non-precious metal oxides, more active sites can be exposed to improve the catalytic activity in EG oxidation. However, some intermediates or impurities may be formed during the oxidation of EG. Compared with precious metal catalysts, non-precious metal electrocatalysts have relatively strong anti-poisoning ability to some impurities or intermediates that may lead to catalyst poisoning, and can maintain better catalytic activity. The research on selective electrooxidation of small alcohols[51–53] with abundant and cheap iron group metal (Fe, Co and Ni)-based catalysts is noteworthy. Catalysis based on iron group metals (Fe, Co and Ni) often converts to the corresponding acidic products with high FE.

4.1.1 Ni-based catalyst. The Ni-based catalyst has a unique electronic structure, and the unfilled d-orbital can form a strong chemical bond with the reactant molecules (such as EG), thereby promoting the reaction. In the oxidation reaction, the Ni-based catalyst can also effectively activate the C–H and O–H bonds in the EG molecule, making it easier to oxidise. Liu *et al.*[54] synthesised Co-Ni_3N/CC nanosheets supported on carbon cloth. As a bifunctional electrocatalyst, the electrode material had a stable crystal structure and excellent EGOR activity. LSV (Fig. 6a) test results showed that the Co-Ni_3N/CC catalytic electrode gave priority to low voltage to achieve high current density in the actual reaction process. It has obvious advantages over OER. Fig. 6b shows that the current density achieved by the EGOR reaction at the same voltage was much higher than that of the OER reaction. Fig. 6c reflects the faster reaction kinetics in EGOR. At a low cell voltage of 1.46 V, the current density of the EGOR anode and hydrogen evolution cathode cell can reach 60 mA cm^{-2}. The *in situ* Raman technique was used to monitor EGOR and indicated that the main active species was NiOOH. At the same time, the DFT calculation results showed that Co-Ni_3N/CC has better adsorption energy and Gibbs free energy change for EGOR. The adsorption capacity of the catalytic electrode for EG is not only influenced by the composition of the material, but also by the structure of the material. For example, Li's[45] research group prepared Ni selenide nanostructures of different shapes and crystalline phases. Due to the different original feed ratios in the synthesis process, the crystal structures were different, which led to different performances of the electrocatalytic oxidation of EG. Compared with the spherical structure and beam structure, the branch structure electrode had higher conductivity and lower charge transfer resistance. Not only that, such a high surface coverage of the active species also greatly improved the catalytic performance of the catalyst. In Fig. 6d, the existence of the orthorhombic system was first confirmed by high-resolution transmission electron microscope (HRTEM) and electron diffraction analysis. The details of the orange square region and its corresponding power spectrum reveal the presence of the $NiSe_2$ cubic lattice in this sample. The elec-

 This journal is © The Royal Society of Chemistry 2025

Published on 12 d'abril 2025. Downloaded on 14/2/2026 0:11:27.

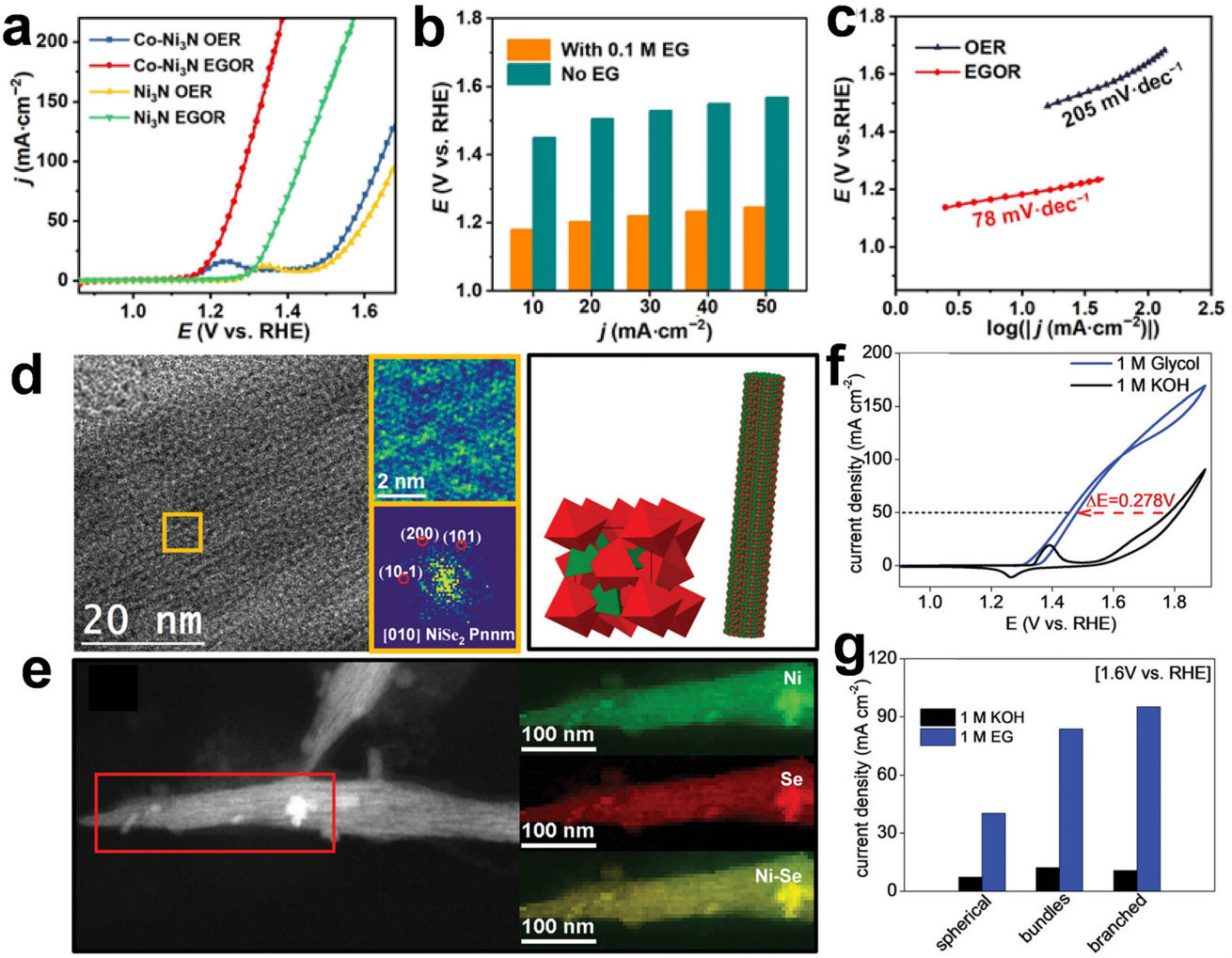

Fig. 6 (a) LSV curve, (b) Co-Ni_3N/CC was tested in 1 M KOH with 0.1 M EG and 1 M KOH without 0.1 M EG, respectively, (c) Tafel diagram with different current densities, reproduced with permission.[54] Copyright 2022, Springer Nature. (d) HRTEM image of $NiSe_2$ branching, the details of the orange square region and its corresponding power spectrum as well as the $NiSe_2$ unit crystal model of the black square region and the three-dimensional atomic supercell model of the $NiSe_2$ beam, (e) the EELS chemical composition map, (f) CV curve for electrodes based on branched $NiSe_2$ particles in 1 M KOH with and without 1 M EG, (g) the current density of the $NiSe_2$-based electrode at 1.6 V is relative to the current density in 1 M KOH with and without 1 M EG, reproduced with permission.[45] Copyright 2023, John Wiley and Sons.

tron energy loss spectroscopy (EELS) chemical composition map (Fig. 6e) shows that Ni and Se were uniformly distributed within each particle. As shown in Fig. 6f, the LSV results showed that the branched $NiSe_2$ nanoparticles had the best performance, with a current density of up to 96 mA cm^{-2} in the electrolyte containing 1 M KOH and 1 M EG at 1.6 V. Fig. 6g shows that the electrode material exhibited higher catalytic activity in EGOR compared with the OER in a three-electrode system. In the same year, Liu *et al.*[55] synthesised the Ni $(OH)_2$/NF electrocatalyst. Fig. 7a shows the XRD test results. The successful synthesis of the catalytic electrode showed that the catalyst had excellent electrocatalytic activity and achieved high current density at medium potential; Fig. 7b and c show that the catalyst had a high FE of formate (93.2%) and selectivity (96%) at high current density. The reaction pathway and mechanism of EG oxidation were investigated by combining *in situ* electrochemical Raman spectroscopy, *in situ* electrochemical Fourier transform infrared spectroscopy and nuclear magnetic resonance spectroscopy. It was further demonstrated that the large amount of NiOOH substance formed *in situ* was the actual active substance for the EG reaction, thus revealing effective EGOR activity.

4.1.2 Co-based catalyst. The cobalt-based catalyst also has high catalytic activity for the oxidation of EG, which can effectively promote the chemical bond cleavage and oxidation reaction in EG molecules under relatively low temperature and pressure conditions, and improve the reaction rate and efficiency. Ma *et al.*[36] investigated the oxidation performance of EG on a Co electrode. The catalytic activity of the electrode was investigated by varying the concentration of EG in the electrolyte. For Co and Ni electrodes, the oxidation reaction of EG occurs in alkaline electrolyte, and the reactive sites are usually

Published on 12 d'abril 2025. Downloaded on 14/2/2026 0:11:27.

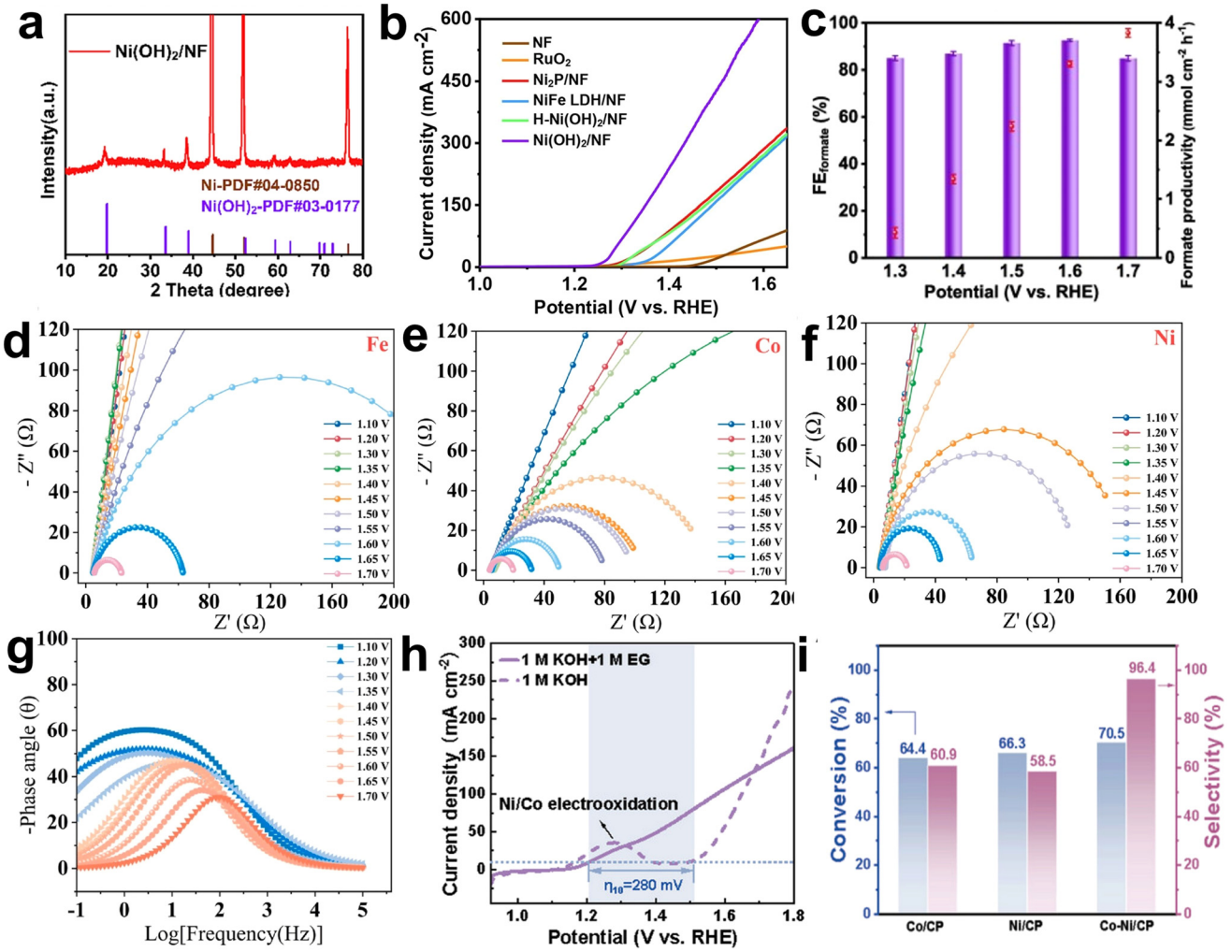

Fig. 7 (a) XRD pattern of $Ni(OH)_2$/NF, (b) LSV curve in EGOR reaction, (c) LSV curve, reproduced with permission.[55] Copyright 2023, Elsevier. (d) The electrochemical impedance spectra of Fe electrodes in 1 M NaOH with 1 M EG at different potentials, (e) the electrochemical impedance spectra of Co electrodes in 1 M NaOH with 1 M EG at different potentials and (f) the electrochemical impedance spectra of Ni electrodes in 1 M NaOH with 1 M EG at different potentials, and (g) the corresponding Bode phase diagram of Co, reproduced with permission.[36] Copyright 2023, Elsevier. (h) LSV curves for EGOR, (i) conversion rates (EG) and selectivity (GA) for Co/CP, Ni/CP and Co–Ni/CP. Co–Ni/CP had the highest EG conversion (96.3%) and GA selectivity (70.6%), reproduced with permission.[56] Copyright 2024, John Wiley and Sons.

high-valence metal sites, which means that EGOR can easily occur at Co^{4+} and Ni^{3+} sites (or CoO_2 and NiOOH sites). Fig. 7d–f show the electrochemical impedance diagrams of the three metals, and when the applied potential reaches 1.60, 1.40, and 1.45 V, respectively, the Fe, Co, and Ni electrodes appear to be clearly semicircular, which indicates that EG oxidation reaction starts to take place. At the occurrence of EGOR, the Co electrode has the lowest reaction potential, and the evolution of the reaction kinetics and phase angle with frequency is consistent with the description of the g-bode phase diagram in Fig. 7, where the decrease of the peak intensity at higher potentials indicates that the electrode facilitates the acceleration of the interfacial charge transfer. When the potential exceeded 1.40 V, the peak position of the Co electrode gradually shifted to higher frequencies and the intensity was significantly weakened, indicating that the surface metal oxidation was accelerated, which led to the rapid oxidation of EG. Thus, these results further confirm that high-valence species are essential for fast EGOR. On this basis, a cobalt–Ni metal composite, Co–Ni/CP,[56] was reported, in which high-valent CoOOH species were generated during the initial oxidation process and acted as the main active center for EG oxidation and could be used as a highly active bifunctional catalyst. Meanwhile, the Ni site has a promoting and stabilizing effect on the active species Co ~(3+), which enhances the reaction rate of EGOR, and Fig. 7h also reveals the excellent catalytic performance of this catalyst compared with the OER. Not only that, Fig. 7i shows that high conversion (>86%) and selectivity (96.3%) can be achieved at high current density (160 mA cm^{-2}) for this electrode, which is almost the best among the reported non-precious metal catalysts, providing valuable insights into the mechanism of EGOR with non-precious catalysts. Zhou's[7]

This journal is © The Royal Society of Chemistry 2025

Published on 12 d'abril 2025. Downloaded on 14/2/2026 0:11:27.

research team synthesised a series of Co and Ni phosphides supported on Ni foam (NF) by serial EG properties. *In situ* electrochemical Raman spectroscopy and synchrotron radiation spectroscopy verified the actual active species in this reaction. As shown in (Fig. 8a) EDS, the three elements are evenly distributed. In the $CoNi_{0.25}P$ material, Ni_2P particles and CoP particles combine to form a CoP–Ni_2P heterojunction, which regulates the electronic structure of the catalyst. The electron movement between the interfaces facilitates the conversion of phosphide into the active material of EG electrocatalytic oxidation, and at the same time reduces the charge transfer resistance to accelerate the electron transport rate and improve the catalytic activity of the catalyst.[57] Fig. 8b shows that the CoP–Ni_2P catalyst has excellent catalytic activity in an electrolyte containing 0.3 M EG and 1 M KOH, and the initial potential moves to a lower potential (1.22–1.33 V *vs.* RHE) compared with the OER. As shown in Fig. 8c, $CoNi_{0.25}P$/NF achieves 91.7% FE formate and 4.1 mmol cm^{-2} h^{-1} formate yield at a commercially relevant current density of ~360 mA cm^{-2} at 1.8 V (*vs.* RHE). In the reaction process, the active

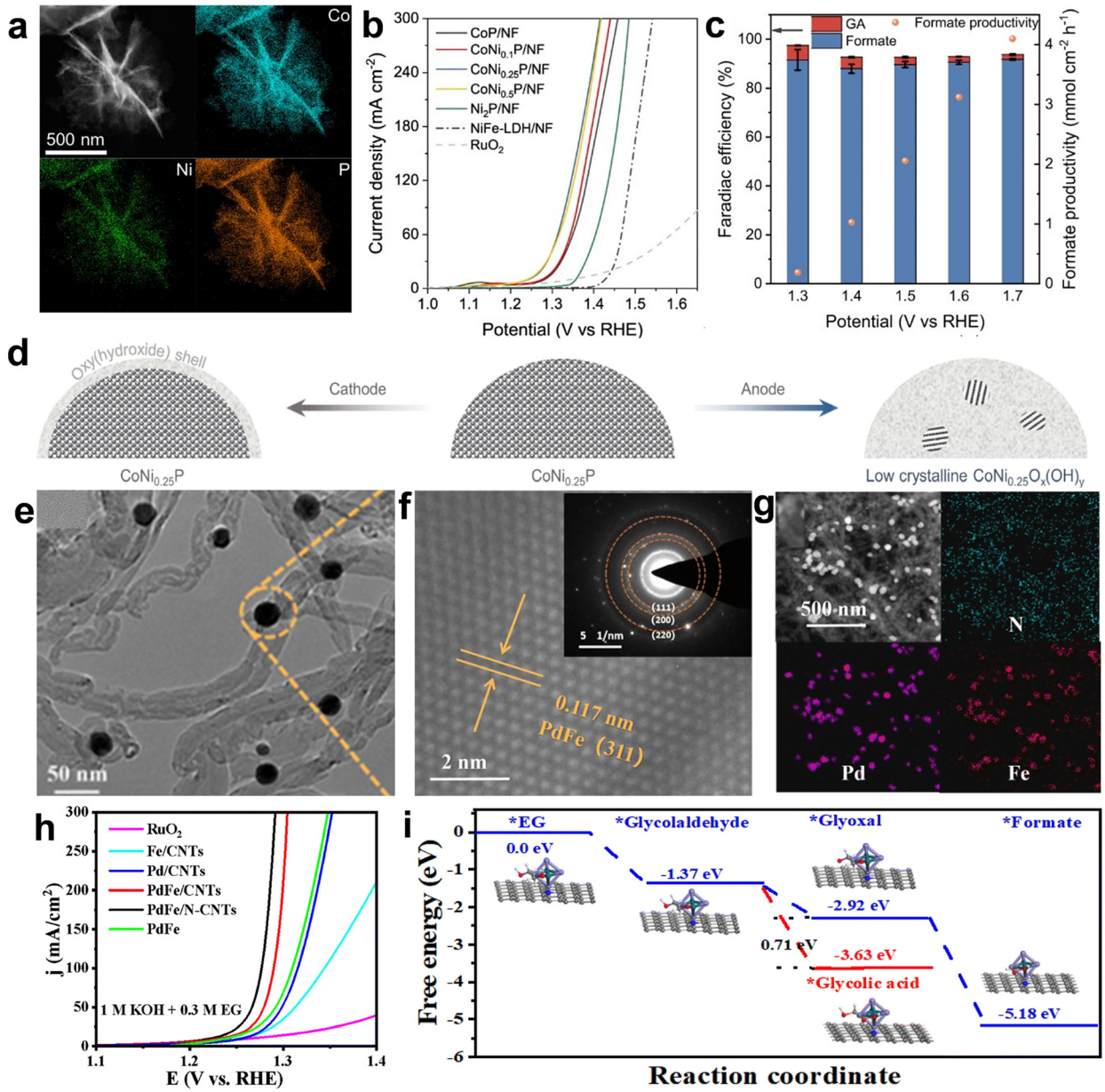

Fig. 8 (a) EDX element map of $CoNi_{0.25}P$, (b) LSV curve of $CoNi_{0.25}P$ in EGOR reaction, (c) FE and formic acid productivity of $CoNi_{0.25}P$/NF at different potentials, (d) schematic diagram of the structural evolution of $CoNi_{0.25}P$ catalyst under reaction conditions, reproduced with permission.[7] Copyright 2021, Springer Nature. (e) HRTEM image of PdFe/N-CNT, (f) HRTEM image of PdFe/N-CNT, (g) mapping of Pd, Fe, N and C corresponding elements of PdFe/N-CNT (h) LSV graph of EGOR of PdFe/N-CNT, (i) free energy of EG on PdFe/N-CNT catalyst, reproduced with permission.[59] Copyright 2024, Royal Society of Chemistry.

Published on 12 d'abril 2025. Downloaded on 14/2/2026 0:11:27.

material is a high-valence metal species and there is a surface reconstruction phenomenon similar to the OER reaction, which is also confirmed by *in situ* Raman spectroscopy. As shown in Fig. 8d, the $CoNi_{0.25}P$ material evolved into a $CoNi_{0.25}P/CoNi_{0.25}O_x(OH)_y$ core–shell structure at the cathode, which was rapidly oxidised at the anode and reconstituted into low-crystallinity $CoNi_{0.25}P/CoNi_{0.25}O_x(OH)_y$ to achieve efficient oxidation of EG.

4.1.3 Fe-based catalyst. There are not many studies on the electrooxidation of EG for iron-based catalysts, but it has been studied by many researchers due to its low cost. The alloy of metallic iron and other metals is a good control strategy, and the unique interfacial structure regulates the electronic structure of the catalyst, so that the catalyst can efficiently electrocatalyse the oxidation of EG to produce efficient oxidation products. However, it is worth noting that it still has very big advantages over other non-precious metals except Ni and Co-based catalysts. The iron-based catalyst has a variety of variable oxidation states that can participate in the reaction process and promote the chemical bond breaking and oxidation reaction in EG molecules. Sun *et al.*[58] found that Fe_3O_4 is highly dispersible in glycol solution and investigated its EG oxidation performance. Experiments showed that when Fe_3O_4 acts as a catalyst, the oxygen atom of PET can combine with Fe^{2+} and Fe^{3+}, making the carbon atoms on the carbonyl group more electron deficient, making it easier for the oxygen atoms in EG to attack the carbonyl group and form an unstable transition. In the same year, Zhang *et al.*[59] found that the PdFe/N-CNT mixed catalysts can be employed to electrocatalyse the conversion of PET waste to valuable formate and hydrogen efficiently and selectively. As shown in Fig. 8e and f, the scanning electron microscope (SEM) and transmission electron microscope (TEM) images of PdFe/N-CNT, respectively, reveal that many well-dispersed spherical nanoparticles are uniformly fixed on the surface of the N-CNT networks. Fig. 8g also shows the elements uniformly dispersed on the substrate material, demonstrating the successful synthesis of the catalyst. Fig. 8h shows that in the mixed solution of 1 M KOH and 0.3 M EG, the catalyst exhibits significant electrocatalytic oxidation activity towards EG in alkaline medium. When the current density reaches 10 mA cm^{-2}, only 1.22 V is required and 86.7% formate selectivity and 87% Faraday efficiency can be achieved. The PdFe/N-CNT catalyst also showed a lower Tafel slope (64.3 mV dec^{-1}), indicating that the reaction kinetics of the PdFe/N-CNT catalyst was better for EGOR. DFT calculation shows that, as shown in Fig. 8i, the Fe inclusion in PdFe/N-CNT helps to regulate the electronic environment and improve the charge distribution around the Pd atoms, which contributes to the enhanced electrocatalytic activity of PdFe/NCNT, which has an important effect on the adsorption of EG* and OH* on the catalyst surface and the performance of EGOR. The adsorption energies of EG* and OH* on PdFe/N-CNTs and Pd/N-CNTs were calculated based on the optimised adsorption model, which further explained the dominant role played by the Fe atom. Lei's[60] group continued to study the oxidation activity of Fe-based catalyst in EGOR. As shown in Fig. 9a and b, Fe atoms were oxidized after electrochemical tuning and their valence states were increased from the original 0 and +2 to +3. In addition, the electrochemical surface area (ECSA) was increased by 86% after the introduction of Fe atoms, as shown in Fig. 9c, suggesting that the presence of Fe effectively enhanced the activity of the catalyst. From the analysis, it can be seen that ET-Pt–Fe has the highest current density and the slowest decay rate. This is because the D-band centre of Pt is shifted down by compressive strain, thereby weakening the adsorption of CO on ET-Pt–Fe and improving its CO oxidation capacity. Fig. 9d further illustrates the stability of the material. After the reaction, Pt/C and PT-Fe decay rapidly to 0.84 A mg cm^{-2} and 0.04 A mg cm^{-2} while ET-Pt–Fe still has a retention rate of 29.1% after 66 hours.

4.1.4 Other electrocatalysts. In addition to Ni, Co and Fe-based catalysts, the catalytic activity of Cu-based catalysts for organic oxidation has been investigated. Wang *et al.*[61] found that the CuO NW electrode has high catalytic activity for EG oxidation, achieving 86.6% formate product selectivity and 88% EG conversion Faraday efficiency. The results of product analysis and DFT calculation showed that the optimal reaction pathway is the formation of glyoxal intermediates and formic acid by C–C bond cleavage. As shown in Fig. 10a, SEM images show that CuO nanowires grow uniformly on the surface of the Cu substrate, and the structure of the annealed sample becomes curved and rough, which allows a greater active area to participate in the reaction during the actual reaction. TEM images further showed that the treated nanowires had a coarser structure, and the lattice spacing confirmed the successful conversion of Cu hydroxide to Cu oxide. In Fig. 10b, the voltametric characteristic curve shows that the Cu-based catalyst has a relatively low initial oxidation potential in PET hydrolysates. At a potential of 1.38 V, the current density of the EGOR is 10 mA cm^{-2}. Fig. 10c shows that the CuO NW-200 °C electrode has a low Tafel slope of 96 mV dec^{-1} and an initial potential of 1.26 V, indicating excellent electrocatalytic activity and a fast reaction rate towards EGOR. The products in the reaction process were monitored and it was found that the EG conversion rate reached 94%, as shown in Fig. 10d and e. The reason why the Faraday efficiency of the product does not reach 100% is mainly due to the occurrence of formate mineralisation during electrolysis. However, this does not affect the product selectivity of the Cu-based catalysts. To further confirm the selectivity of the catalyst, the possible intermediates and products of the reaction were electrolysed at different potentials and determined by high-performance liquid chromatography (HPLC) (Fig. 10f). Cu-based nanowire electrode has formate products >80% at an applied potential of <1.6 V, but the Faraday efficiency of formic acid production decreases significantly when the applied electrolytic potential is 1.66 V. This is due to deep oxidation of formate or water oxidation, but does not affect the highly selective oxidation of EG by Cu-based catalysts. More than just Cu-based catalysts, Wang's[44] team reported a catalyst based on amorphous MnO_2, and Fig. 10g and h show the successful synthesis of this electrode

 This journal is © The Royal Society of Chemistry 2025

Published on 12 d'abril 2025. Downloaded on 14/2/2026 0:11:27.

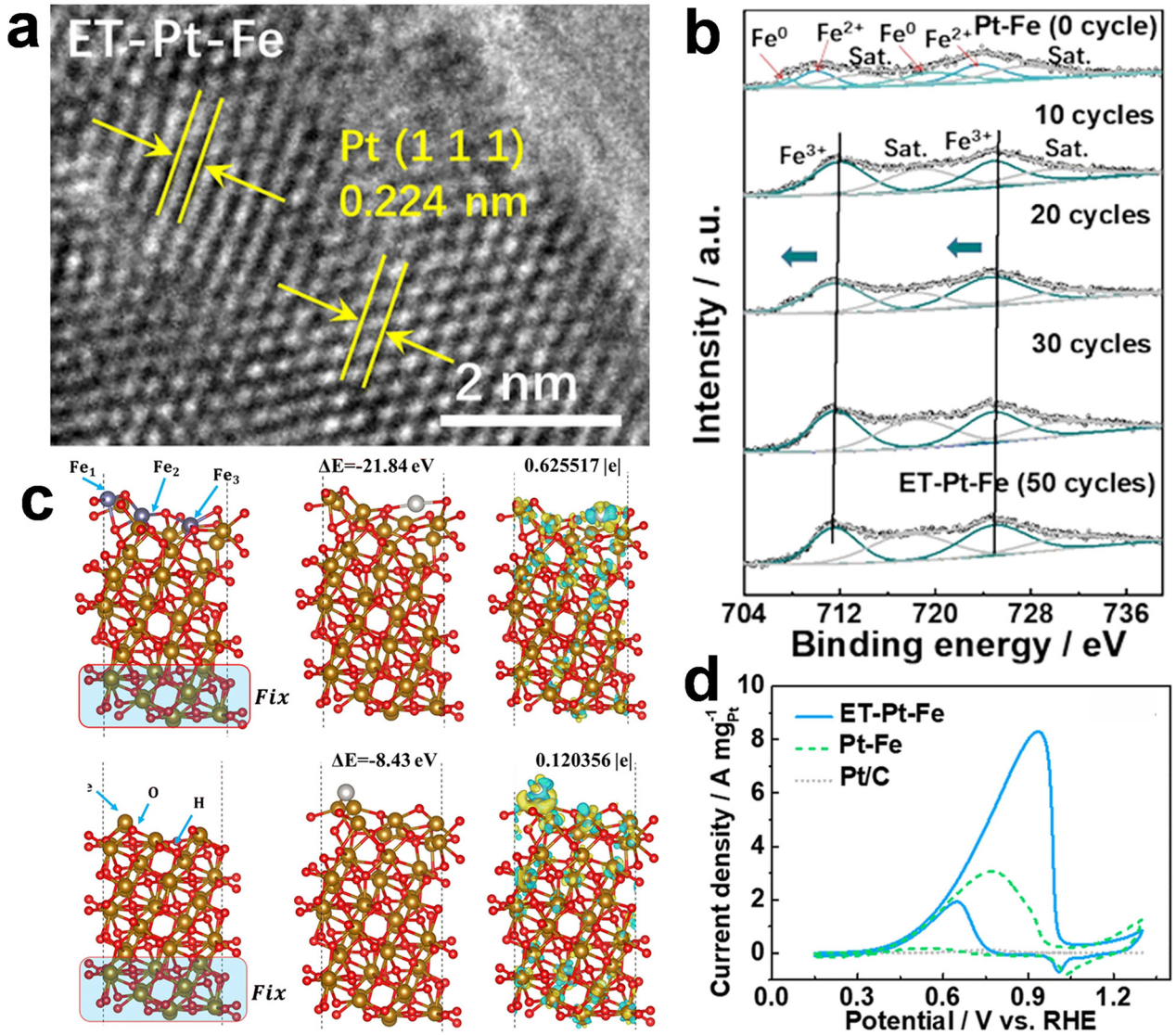

Fig. 9 (a) HRTEM image of ET-Pt–Fe, (b) XPS image of Fe element, (c) from left to right: there are three different Fe vacancies on the surface of Fe_2O_3(112) (yellow, red, silver and purple circles represent Fe atom, O atom, Pt atom and Fe vacancy, respectively), the adsorption energy of Pt atom on Fe_2O_3(112) surface with Fe^{3+} vacancy, the charge density difference of Pt atom on Fe_2O_3(112) crystal surface, Fe_2O_3 three adsorption sites on the (112) crystal plane, the adsorption energy of Pt atoms on the surface of Fe_2O_3(112), the charge density difference of Pt atoms adsorbed on the surface of Fe_2O_3(112), (d) Pt/C, Pt–Fe and ET-Pt–Fe in solution at 60 mV s^{-1} CV curve, reproduced with permission.[60] Copyright 2024, Royal Society of Chemistry.

material. For EGOR, Mn-OH_{ads} species formed on a-MnO_2 can remove CO_{ads}, thereby improving charge transfer and stability. At the same amorphous MnO_2 is conducive to the regulation of electronic structure. This is because the interaction between Pd and a-MnO_2 causes Pd ions to lose electrons to form a hypervalent state species, and this change in electronic structure will lead to the reduction of the activation barrier of the EGOR reaction, thus obtaining excellent EG electrocatalytic oxidation performance.

As shown in Fig. 10i, after 100 cycles, it was observed that the current density of Pt/C decreases significantly, and the current density of Pd nanoparticles decreases sharply. The decrease in current density may be due to the presence of toxic species and intermediates, resulting in a decrease in active centers. It was found that Pd/a-MnO_2 decay rate was relatively slow, which also confirmed that the presence of MnO_2 reduced the adsorption of toxic species and intermediates on the catalyst surface, thus improving the stability of the catalyst.

4.2 Precious metal catalysts

It is well known that the catalytic activity of non-precious metal catalysts is relatively low, but in recent years, the research on non-precious metal catalysts has made continuous progress, and the activity of some new non-precious metal catalysts has been gradually improved. Carbide, nitride, and

Published on 12 d'abril 2025. Downloaded on 14/2/2026 0:11:27.

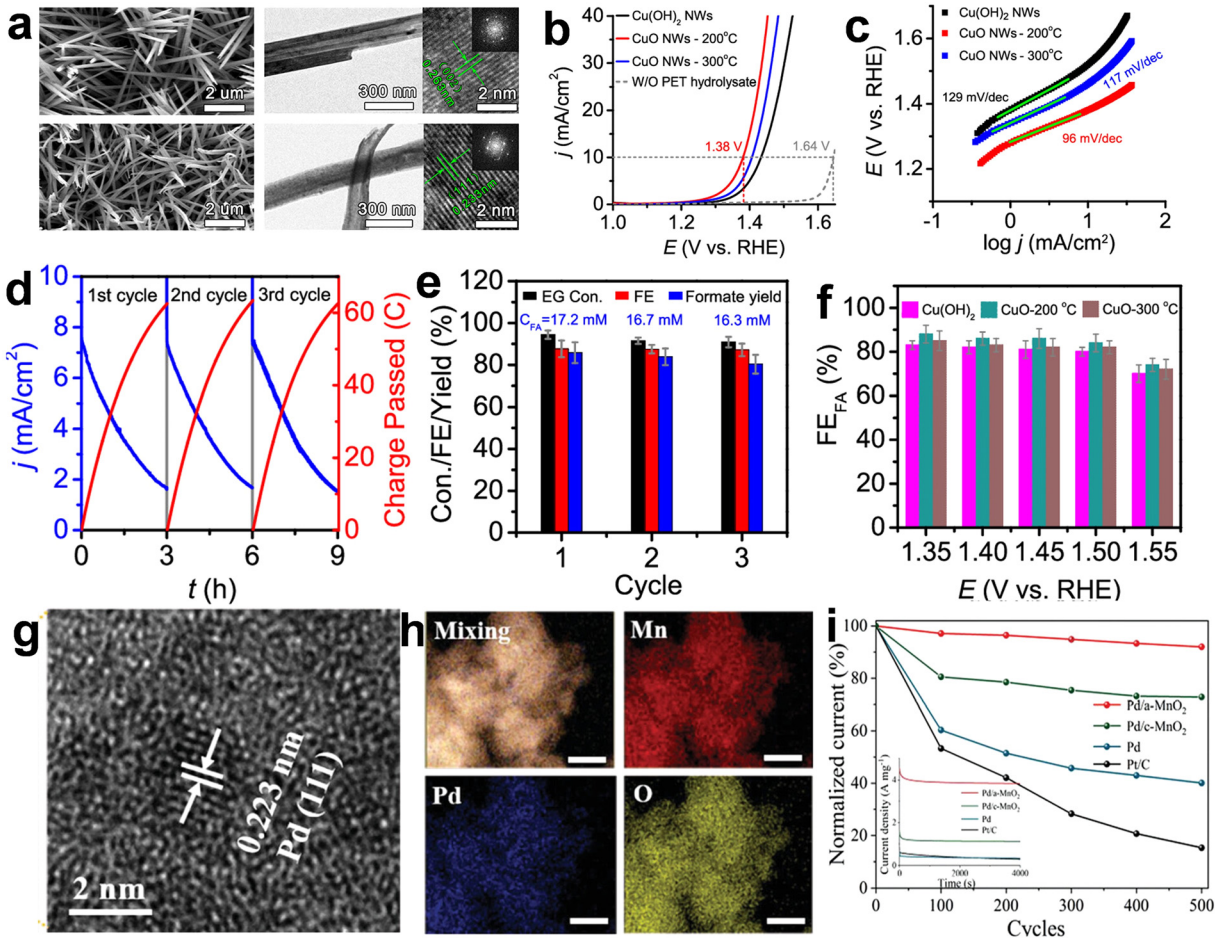

Fig. 10 (a) SEM image (top left and bottom left) of $Cu(OH)_2$ NW and TEM (top right) HRTEM image of CuO NW at −200 °C (bottom right), (b) LSV curve, (c) of $Cu(OH)_2$ and CuO NW electrodes at a potential of 1.40 V In the mixture of 0.1 M KOH with EG, (d) the curve of the current time and charge accumulation time of electrolysis at 1.46 V, (e) the corresponding EG conversion rate, Faraday efficiency and formate yield, (f) the Faraday efficiency of formate on different electrodes at different electrolytic potentials, reproduced with permission.[61] Copyright 2022, American Chemical Society. (g) HRTEM image, (h) corresponding element mapping diagram of Pd/a-MnO_2, (i) comparison diagram of catalyst durability curve in EGOR reaction, the illustration is a current–time chrono ampere-graph of Pd/a-MnO_2, Pd/C-MnO_2, Pd and Pt/C for 4000 s at 0.8 V in 1 M KOH with 0.6 M EG, reproduced with permission.[44] Copyright 2023, John Wiley and Sons.

sulfide non-precious metal catalysts can also show certain catalytic activity under specific conditions. Because of the scarcity and high value of the precious metals themselves, and their high preparation cost, which limits the extensive use of precious metal catalysts in large-scale industrial applications, vigorous efforts have been made to develop more abundant non-precious metal catalysts for EG electrocatalytic oxidation reactions. However, the high activity of noble metals in the electrochemical oxidation reaction of EG is undeniable. For example, the d electron orbitals of noble metals, such as Pt and Pd, are not filled, and it is easy to adsorb reactants on the surface; the strength of adsorption is moderate, which is conducive to the formation of the intermediate 'active compounds', and can promote the electrocatalytic oxidation of EG more efficiently. Secondly, the precious metal more easily adsorbs reactants on the surface than the other metals. Thirdly, compared with non-precious metals, noble metals have higher selectivity, which can more effectively control the reaction in the direction of the target product and reduce the occurrence of side reactions. Therefore, exploring how to efficiently utilize precious metal catalysts is also an issue of concern. Research into precious metal catalysts for EG oxidation initially focused on the elemental precious metals. Among them, Pt, Pd,[62] Rh and other noble metals show some catalytic activity due to their unique electronic structure and chemical properties The unique electronic structure of precious metals has a key effect on the performance of electrocatalytic oxidation of EG, which is mainly reflected in three key aspects: D-band centre location, electron orbital hybridization and electron cloud distribution. The location of the centre of the d band plays an important role in the adsorption capacity and the detachment of the reaction intermediates. The degree of its proximity to the Fermi level determines the interaction strength between the precious metal atoms and the adsorbents. The appropriate location can promote the adsorption and activation of EG, ensure the smooth progress of the reaction, and ensure the

 This journal is © The Royal Society of Chemistry 2025

Published on 12 d'abril 2025. Downloaded on 14/2/2026 0:11:27.

timely desorption of the intermediates to prevent them occupying the active site and hindering the subsequent reaction. Electron orbital hybridization affects the charge transfer between catalyst and reactant. Reasonable hybridization can optimize the electron cloud distribution and migration ability, accelerate the charge transfer and enhance the reaction activity. At the same time, in alloys or complexes, the synergies brought about by hybridization can further optimize the active site and enhance the catalytic performance. The electron cloud distribution affects the contact between the reactant and the catalyst active site through the steric hindrance effect. Too dense an electron cloud will prevent EG from approaching the active site and reduce the reaction rate, while an appropriate electron cloud distribution can reduce the hindrance and increase the reaction rate. In addition, it also determines the selectivity of the reaction, and different electron cloud distributions give the catalyst a preference for different reaction paths, and then affect the product distribution. However, research during this period has mainly focused on the simple noble metal catalyst, and the understanding of its catalytic performance is still relatively preliminary; for example, using simple Pt black as a catalyst, the catalytic efficiency is relatively low and the stability needs to be improved. With the development of nanotechnology, researchers began to pay attention to the effect of the morphology of noble metal catalysts on their catalytic performance. By controlling the synthesis methods and conditions, noble metal nanomaterials with different morphologies, such as nanoparticles, nanorods, nanowires and nanosheets, have been prepared. These nanomaterials with different morphologies have different specific surface areas, surface energies and electronic structures, which affect their catalytic performance for glycol oxidation. For example, the nanoflake Pt catalyst showed higher catalytic activity than the nanogranular Pt catalyst in EG oxidation due to its large specific surface area and special electronic structure. To further improve the performance of precious metal catalysts, researchers have begun alloying precious metals with other metals. Alloying can change the electronic structure and lattice parameters of precious metals, thereby improving their catalytic activity and stability. For example, the catalytic performance of Pt for EG oxidation has been improved by forming alloys with Cu, Ni and other metals to take advantage of the electronic and synergistic effects of Cu and Ni. In addition to binary, ternary or even multi-component noble metal composite catalysts, multi-metal composite catalysts have gradually become the focus of research. These multi-metal composite catalysts can combine the advantages of multiple metals and further improve the catalytic performance of EG oxidation through synergistic effects. There are studies on the preparation of Pt–silver–Cu ternary nanosheet assembly, which shows excellent electrocatalytic performance in EG oxidation reaction, and the mass activity is far more than that of monometal and binary catalysts. The following is a summary of several precious metal catalysts.

4.2.1 Pt-based catalyst. Jin *et al.*[63] synthesized Pt–Au alloys, demonstrating the excellent performance of precious metal catalysts for EG oxidation. Pt was deposited on the surface of the polycrystalline Au electrode by electrodeposition, and the presence of Pt indeed improved the activity of the catalyst, because Pt provides a large number of reaction sites for oxidation and thus increases the reaction rate. Previous work has shown that the peak current density of the Pt electrode is higher than that of the Au electrode in the electrocatalytic oxidation of EG under alkaline conditions, and conversely, the peak current density of the Pt electrode is lower than that of the Au electrode. As can be seen from Fig. 11a, due to the presence of Pt, the peak potential of the electrode shifts negatively by about 0.46 V, and the peak current density also increases significantly, which further indicates that Pt significantly improves the catalytic activity of the catalyst. Pu *et al.*[64] constructed a core–shell structure catalyst for the oxidation reaction of EG. Among them, the structure of alloyed Pt–M nuclei could better regulate the electronic effect and showed excellent stability in the electrocatalysis process. Fig. 11b is a typical TEM image of a PtCu/PtCu core–shell tripod, indicating that the catalyst has a stable tripod structure. After CV test, ECSA values of different catalysts were obtained (Fig. 11c and d). Compared with other samples, the samples after the introduction of Pt had a larger ECSA value. This may be due to the fact that the unique structure of the catalyst provides abundant active centres for the catalytic reaction, thus improving the catalytic activity. The results of chrono current testing showed that the catalyst had excellent stability. The PtCu/Pt_{77}Cu TDNs/C maintained the highest current density for 7200 seconds (Fig. 11e), and retained the maximum specific activity of 8.9 mA cm^{-2} and mass activity of 6.8 A mg^{-1} after the reaction. The Song[65] research group synthesized a single-atom Pt1/Ni$(OH)_2$ electrocatalyst, which showed excellent electrocatalytic oxidation of EG by loading only one millionth part of precious metal Pt. In order to confirm the existence of Pt, the AC HAADF-STEM test proved that Pt elements were uniformly distributed in the composite materials as atoms (Fig. 11f), and did not exist in the form of nanoparticles. The content of Pt was 0.8 wt% as determined by inductively coupled plasma mass spectrometry (ICP-MS). As shown in Fig. 11g, the current density of the sample impregnated for 3 h at voltages greater than 1.4 V was greater than 600 mA cm^{-2}, indicating excellent catalytic activity. In addition, the etching strategy is widely applicable to other Pt group metals, as shown in Fig. 11h and 10i. The synthetic electrodes containing these noble metals all showed good performance in the oxidation of EG, but were slightly less effective than Pt.

4.2.2 Pd-based catalyst. Oscar Ambriz-Peláez *et al.*[66] synthesized Pd-MoO_x nanomaterials for the oxidation of EG. The EGOR activity of the electrode material was tested with 0.3 M KOH as electrolyte, and the concentration of EG was changed from 0.1 to 1 M. The catalytic activity of different materials is shown in Fig. 12a, and a summary of the activity at different EG concentrations is shown in Fig. 12b. It can be seen that the combination of Pd and other materials can indeed improve the activity of the electrode, and appropriate EG concentration is also the key to improving the catalytic activity. Wei *et al.*[11]

Published on 12 d'abril 2025. Downloaded on 14/2/2026 0:11:27.

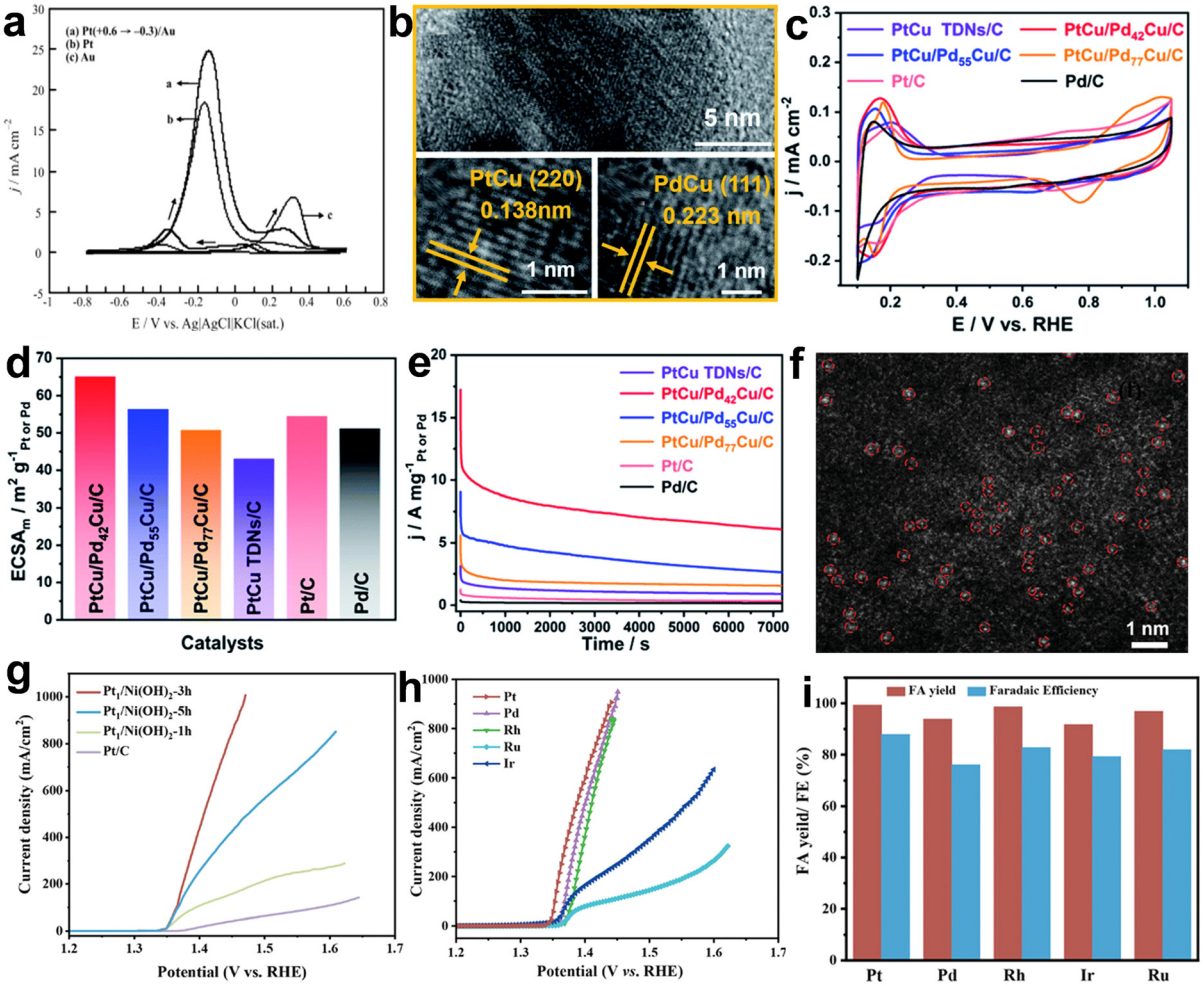

Fig. 11 (a) CV of Pt (+0.6 → −0.3)/Au, Pt and Au electrodes in 0.6 M NaOH with 0.1 M glycol at a scanning rate of 60 mV s^{-1}, reproduced with permission.[63] Copyright 2010, Elsevier. (b) HRTEM images of $PtCu/Pd_{77}Cu$ core–shell TDNs, (c) CV curves of different catalysts at 60 mV s^{-1} scanning rate in the electrolyte, (d) ECSA histogram of different catalysts, (e) *I*–*t* curves of different catalysts in electrolyte solution at 1.0 M KOH with 1.0 M EG, reproduced with permission.[64] Copyright 2022, American Chemical Society. (f) HAADF-STEM images of $Pt/Ni(OH)_2$-3 electrocatalysts, (g) EGOR properties of different samples, (h) and (i) properties of other elements, reproduced with permission.[65] Copyright 2024, John Wiley and Sons.

synthesized PdSb with a rich defect structure to electrochemically convert PET EG into the high-value chemical glycolic acid. P–d orbital hybridization in PdSb bimetal can promote the C–C bond break of EG and the rapid oxidation of –OH, thus enhancing the catalytic performance of PdSb bimetallic alkenes. High-angle toroidal dark-field scanning HAADF-STEM images of PdSb, shown in Fig. 12c, demonstrated the successful preparation of ultra-thin 2D nanosheets. TEM images further confirmed the presence of perforation structures in the nanosheets, which contribute to the transport of electrons and increase catalytic activity. LSV (Fig. 12d) test results showed that when the current density reaches 10 mA cm^{-2}, the required potential of EGOR reaction is 0.9 V lower than that of OER. The activity of PdSb bimetal was obviously better than that of other catalysts. At the optimum potential of 0.76 V, the selection rate of glycolic acid was 92.0% (Fig. 12e), and the Faraday efficiency could reach 93.4% (Fig. 12f). These results all prove that PdSb has excellent properties in EGOR. In addition, the structure of PdSb remained basically unchanged after the reaction, which further indicated that the catalyst had excellent stability.

4.2.3 Rh-based catalyst. As a new element of the Pt group, Rh is widely used in various electrocatalysis fields due to its good catalytic activity and high inherent corrosion resistance. Mao *et al.*[67] applied Rh metal to the *in situ* reconstruction of glycol-assisted seawater cracking. Due to its unique metal structure and Rh/RhOOH heterogeneous structure, Rh/RhOOH metal can perform well in the HER (overpotential 29 mV) and EGOR. Fig. 12g shows the morphology and structure of the electrode material. As shown in Fig. 12h, in the Rh mass normalization and ECSA normalized CV curves, the ECSA of Rh/RhOOH is 60.28 m^2 g^{-1}, which is higher than that of RhOOH NSs (41.72 m^2 g^{-1}), Rh metallene (30.64 m^2g^{-1}) and Pt/C (66.79 m^2 g^{-1}). This indicates that it has more active sites. Fig. 12i shows that in 1 M KOH with 1 M EG solution, Rh/RhOOH also has better electrocatalytic performance for EGOR

 This journal is © The Royal Society of Chemistry 2025

Published on 12 d'abril 2025. Downloaded on 14/2/2026 0:11:27.

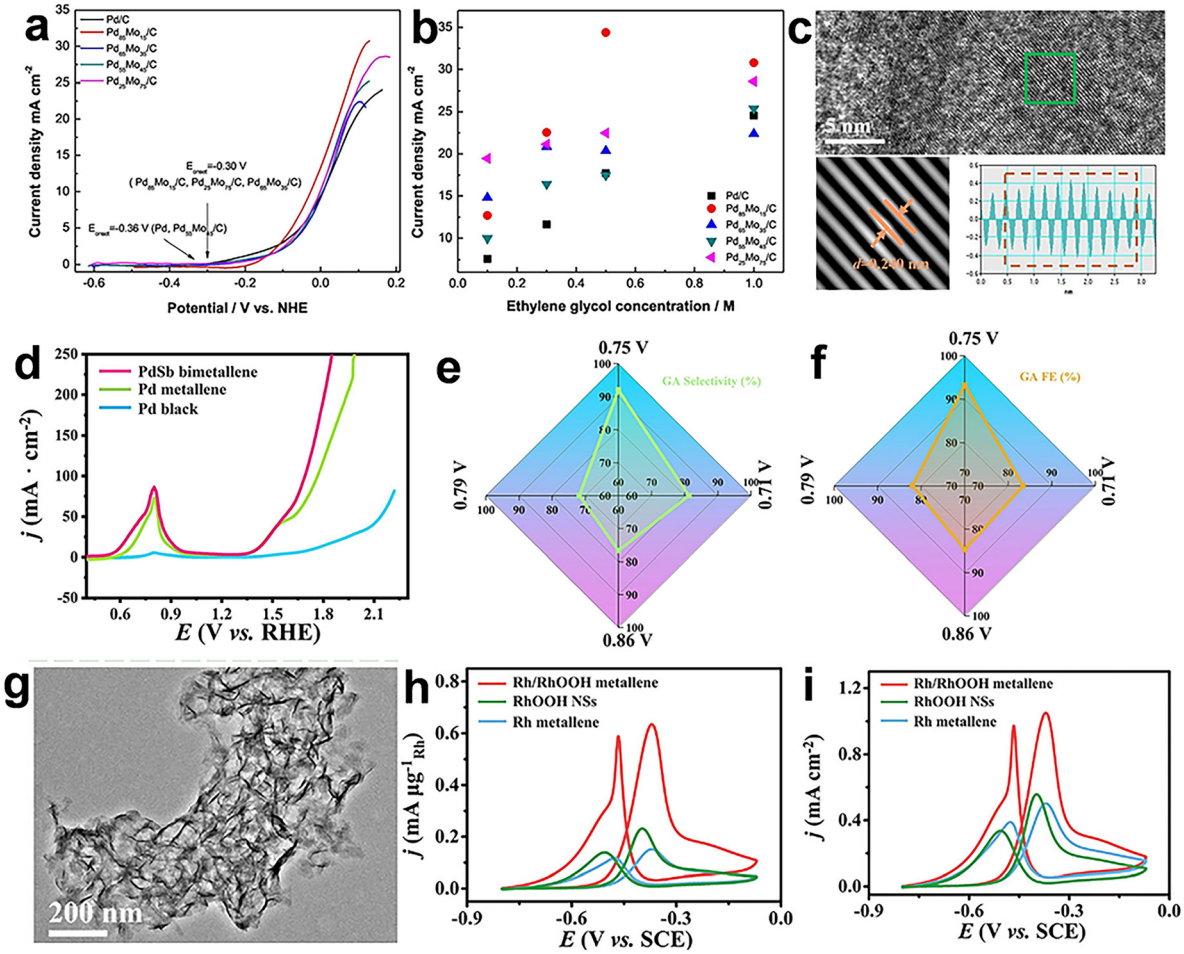

Fig. 12 (a) LSV curves of different electrode materials at 0.3 M KOH as electrolyte and 20 mV s^{-1} as scanning rate activation region, (b) relationship between current density and temperature of Pd/C and Pd-MoO_x materials, reproduced with permission.[66] Copyright 2019, Elsevier. (c) HRTEM image of PdSb bimetal, (d) LSV curve in 0.1 M EG with 1 M KOH solution, (e) selectivity of product in EGOR process, (f) Faraday efficiency of GA, reproduced with permission.[11] Copyright 2024, Elsevier. (g) TEM diagram of Rh/RhOOH, (h) mass normalized CV and (i) ECSA curves of EGOR in N_2-saturated 1 M KOH + 1 M EG solution with different electrocatalysts at a scanning rate of 60 mV s^{-1}, reproduced with permission.[67] Copyright 2022, John Wiley and Sons.

than the comparison sample, with lower initial potential and higher mass activity (MA) and specific activity (SA). The results showed that Rh/RhOOH metal has better electrocatalytic performance for EGOR. Jiang[10] and his team synthesized a PtRh alloyed dendritic nano assembly in which a low concentration of Rh atoms was introduced into the Pt lattice, resulting in tensile strain, which not only improved HER performance but also further improved EGOR reactivity, achieving a current density of 10 mA cm^{-2} with a voltage of only 0.66 V. In this paper, the electrode material in the EGOR-coupled HER reaction was described in detail.

4.2.4 Ru-based catalyst. Ma *et al.*[68] prepared ultra-thin Ni phosphide nanosheet ($Ru/Ni_2P/NF$) nanocomposites modified by ruthenium nanoparticles on a Ni foam matrix. Fig. 13a shows the structure of the $Ru/Ni_2P/NF$ nanoarray. The three elements were evenly distributed, indicating the successful synthesis of $Ru/Ni_2P/NF$. Fig. 13b shows that the oxidation activity of EG was higher after the addition of ruthenium atoms. The oxidation performance of EG of $Ru/Ni_2P/NF$ nanocomposites was tested in an electrolyte containing 0.6 M EG and 1 M KOH, and the initial potential of catalyst was lower than that of the OER. The EGOR response current increased sharply at 1.36 V–1.4 V, which is much higher than the OER. As shown in Fig. 13c, the DFT calculation showed that the adsorption energy of OH^- under different electrocatalyst models. The adsorption energy value of $Ru/Ni_2P/NF$ nanocomposite was −4.32 eV, which was lower than Ru (−3.347 eV) and Ni_2P (−3.609 eV). It was further demonstrated that the adsorption site after the addition of ruthenium could effectively capture EG molecules and promote the oxidation of EG.

Liu *et al.*[78] synthesized a self-supported $Cu(OH)_2$ nanowire array on Cu foam. The $Cu(OH)_2$/CF nanowire array was converted into Cu_xO/CF after solvent heat treatment, showing EGOR electrocatalytic performance. The self-supported nanoarray catalyst h-Ru-Cu_xO/CF, prepared by loading atomic Ru on

Published on 12 d'abril 2025. Downloaded on 14/2/2026 0:11:27.

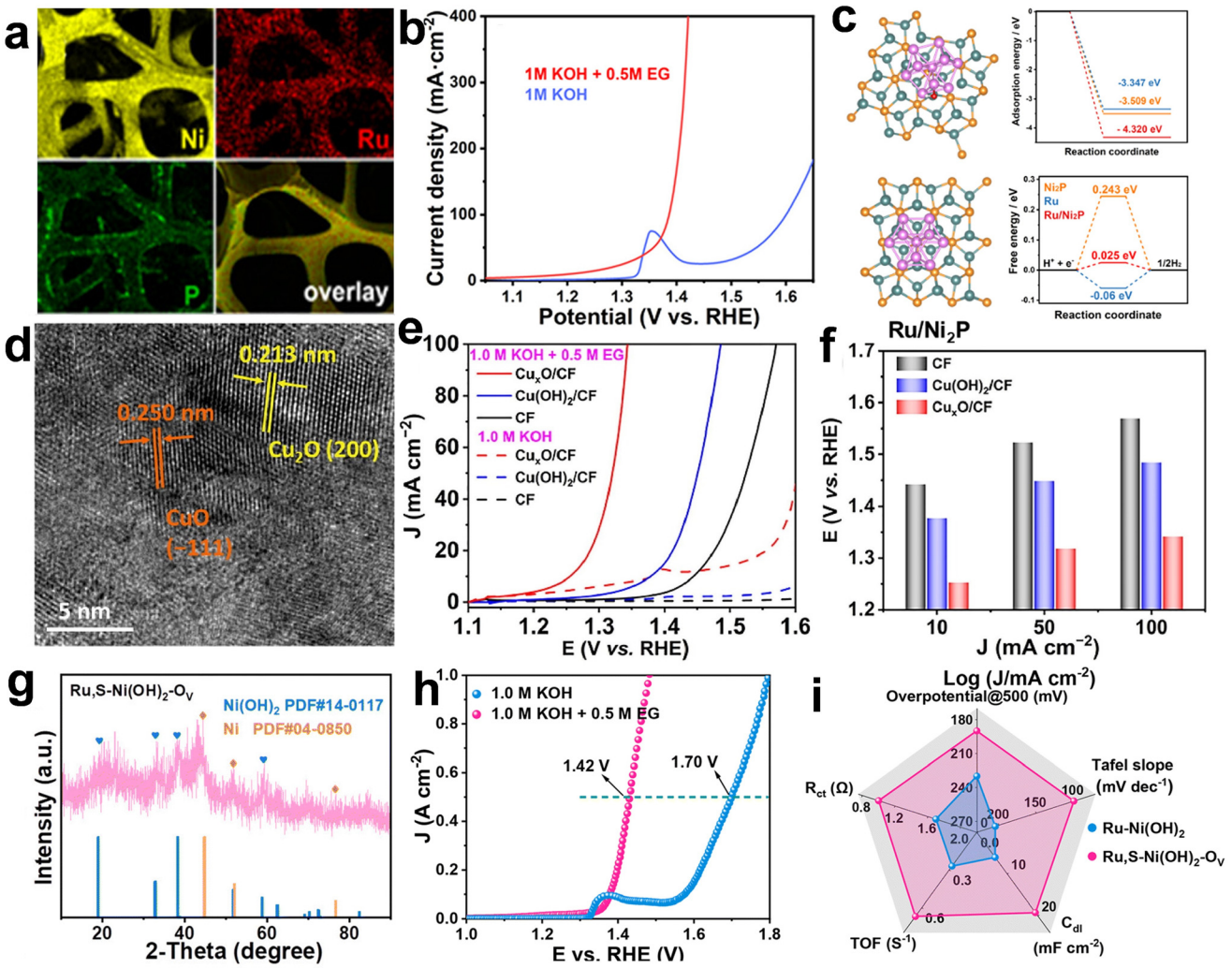

Fig. 13 (a)Element mapping diagram of $Ru/Ni_2P/NF$, (b) LSV curves in 1 M electrolyte containing EG and without EG, the adsorption energy of (c) OH and H* on Ru/Ni_2P catalyst, reproduced with permission,[68] Copyright 2021, American Chemical Society. (d) The high resolution of Cu_2O, the LSV performance comparison diagram of different catalysts, (e) EGOR and OER, (f) the voltage comparison under different current densities, reproduced with permission.[78] Copyright 2023, Elsevier. (g) XRD pattern of Ru, S−Ni $(OH)_2$, (h) comparison of EGOR performance and LSV performance of OER, (i) comparison of various electrochemical parameters of different catalysts radar diagram, reproduced with permission.[69] Copyright 2024, Royal Society of Chemistry.

$Cu(OH)_2$/CF, also showed high electrocatalytic activity in HER. As shown in Fig. 13d, the lattice spacing corresponds to the Cu oxide (2 0 0) and (−1 1 1) crystal faces, respectively, demonstrating the successful synthesis of the substrate material. As shown in Fig. 13e, the initial potential of the electrode material in EGOR reaction was lower than that in OER reaction, and it had better catalytic activity than other catalysts, with higher current density (Fig. 13f) at the same potential. In addition, Cu_xO/CF and h-Ru-Cu_xO/CF were used as anode and cathode to construct a HER// EGOR paired electrolytic system without film. The system could reach the current density of 10 mA cm^{-2} at a voltage of 1.26 V, and was also a difunctional catalyst with excellent performance. Li *et al.*[69] synthesized a Ru- and S-doped Ni hydroxide cross-network structure on Ni foam (NF) by the etching method. The nanoarray structure of Ru, S–$Ni(OH)_2$ could provide more abundant active sites, and the three elements of Ru Ni and O were evenly distributed, which also confirmed the successful synthesis of the Ru, S–$Ni(OH)_2$ electrode materials. XRD results (Fig. 13g) finally proved that the material was successfully synthesized and the current density could reach 1000 mA cm^{-2} (Fig. 13h) at a potential of about 1.4 V in the EGOR reaction. The radar chart (Fig. 13i) also evaluated the excellent activity of the catalyst in terms of impedance and Tafel slope.

Based on the above discussion, the performance of different catalysts in the electrocatalytic EG oxidation reaction is also compared (Table 2), and the performance of different catalysts when coupled with other reactions is further discussed below.

4.3 Application of EGOR with other reactions

The study of coupling EG with other reactions has a green and sustainable application prospect: to develop more efficient cat-

This journal is © The Royal Society of Chemistry 2025

Published on 12 d'abril 2025. Downloaded on 14/2/2026 0:11:27.

Table 2 Comparison between the performances of different catalysts

	Catalyst composition	Microstructure	Electrolyte	Activity, mA cm^{-2}@RHE	Specific surface area	Stability decay (%) @ time	Ref.
Non-precious metal catalyst	Co-Ni_3N/CC	Co-Ni_3N/CC nanosheets loaded on carbon cloth	1 M KOH + 0.1 M EG	1.46 V@60 mA cm^{-2}	78 mV dec^{-1}		54
	$NiSe_2$	Branched $NiSe_2$ nanoparticles	1 M KOH + 1 M EG	1.60 V@96 mA cm^{-2}	—	45.4%@10 h	45
	Co–Ni/CP	Nanoarray structure	1 M KOH + 1 M EG	1.42 V@30 mA cm^{-2}	39 mV dec^{-1}	0@24 h	56
	$CoNi_{0.25}P$/NF	Nanoarray structure	1 M KOH + 0.3 M EG	1.7 V@350 mA cm^{-2}	58.1 mV dec^{-1}		7
	PdFe/N-CNTs	PdFe alloy nanoparticles uniformly dispersed on the surface of N-CNT	1 M KOH + 0.3 M EG	1.28 V@100 mA cm^{-2}	54.3 mV dec^{-1}	~25%@15 h	59
	CuO NW-200 °C	Nanowire structures grown on the surface of Cu substrate	1 M KOH + 0.1 M EG	1.38 V@10 mA cm^{-2}	54.3 mV dec^{-1}	—	61
Precious metal catalyst	$Pt_1/Ni(OH)_2$	Nanoarray structure	1 M KOH + 1 M EG	1.444 V@10 mA cm^{-2}	—	—	65
	PdSb	Nanosheet	1 M KOH + 1 M EG	0.62@10 mA cm^{-2}	—	22.7%@2000 CV	11
	Rh/RhOOH	Nanosheet	1 M KOH + 1 M EG	—	83 mV dec^{-1}	@2.7 h	67
	Ru/Ni_2P/NF	Nanosheet	1 M KOH + 0.5 M EG	1.37 V@100 mA cm^{-2}	—	~42%@10 h	68

alysts, improve the selectivity and conversion of the reaction, and reduce the production of by-products to achieve efficient EG oxidation reaction. For example, coupling the oxidation reaction of EG with the HER of electrolytic water is one of the current research hotspots. In this coupled system, EG, as an organic substrate, undergoes oxidation at the anode, replacing the traditional OER, thereby reducing the overpotential of the anode reaction, improving the efficiency of hydrogen production, and converting EG into valuable chemicals. EG can be electrooxidized to formic acid while producing hydrogen at the cathode.[48,70–76] In this section, EG oxidation and other reaction couplings are discussed.

4.3.1 EGOR coupled with HER. Hydrogen energy as a kind of clean energy has been of interest,[77] and the electrolysis of water to produce hydrogen is a common method. EG oxidation has a lower oxidation potential and can be used as an alternative reaction to the OER to achieve high-efficiency hydrogen production. Jiang *et al.*[10] designed and synthesized Rh atom-modified PtRh nanowires ($PtRh_{0.02}$@RhNWs). The electrode material exhibited excellent performance in both the HER and EGOR and was used as a bifunctional catalyst. This was mainly due to the strain effect of the electrode material induced by interfacial engineering, which further tuned the electrode structure of the material and facilitated the introduction of heteroatomic active centers and the induction of lattice strain, leading to efficient EGOR and HER performance. First, electrochemical tests were performed in 0.1 M KOH solution and 0.1 M KOH seawater solution (pH = 13.8) at a scanning rate of 10 mV s^{-1} in a three-electrode system. The LSV curve shows (Fig. 14a) that when the current density reached 10 mA cm^{-2} in the test process of $PtRh_{0.02}$@Rh nanowires, the overpotential was only 30.6 mV, which is much lower than that of Pt nanowires (99.7 mV) and JM-Pt black (122.3 mV). The Tafel slope value of 39.1 mV dec^{-1} indicated that $PtRh_{0.02}$@Rh nanowires exhibited a faster HER reaction kinetics (Fig. 14b), indicating that the HER process followed the Heyrovsky–Volmer mechanism. Even in industrial application, in 0.1 M KOH electrolyte seawater solution, the overpotential can reach 46.8 mV, and still has excellent HER activity. At the same time, the EGOR property of the electrode material was determined, again in an alkaline seawater solution containing 0.6 M EG. The test results showed that the peak current density of $PtRh_{0.02}$@Rh nanowire EGOR was 1.26 A mg^{-1}, indicating that the electrode had excellent electrocatalytic activity for EG (Fig. 14e). The high mass activity also further indicated that the modification of Rh atoms on the surface of Pt NW effectively improved the catalytic activity of EGOR.

In recent years, researchers have paid more and more attention to the coupling reaction of EGOR and HER. Liu *et al.*[78] constructed a self-supporting nanoarray electrocatalyst h-Ru-Cu_xO, which combined multiple advantages of interface reconstruction and a self-supporting hierarchical structure, and showed excellent catalytic activity during practical testing. The HAADF-STEM image of h-Ru-Cu_xO/CF (Fig. 14d) showed that the catalyst has a hierarchical structure and a rough surface, which both provided abundant active centres and facilitated

Published on 12 d'abril 2025. Downloaded on 14/2/2026 0:11:27.

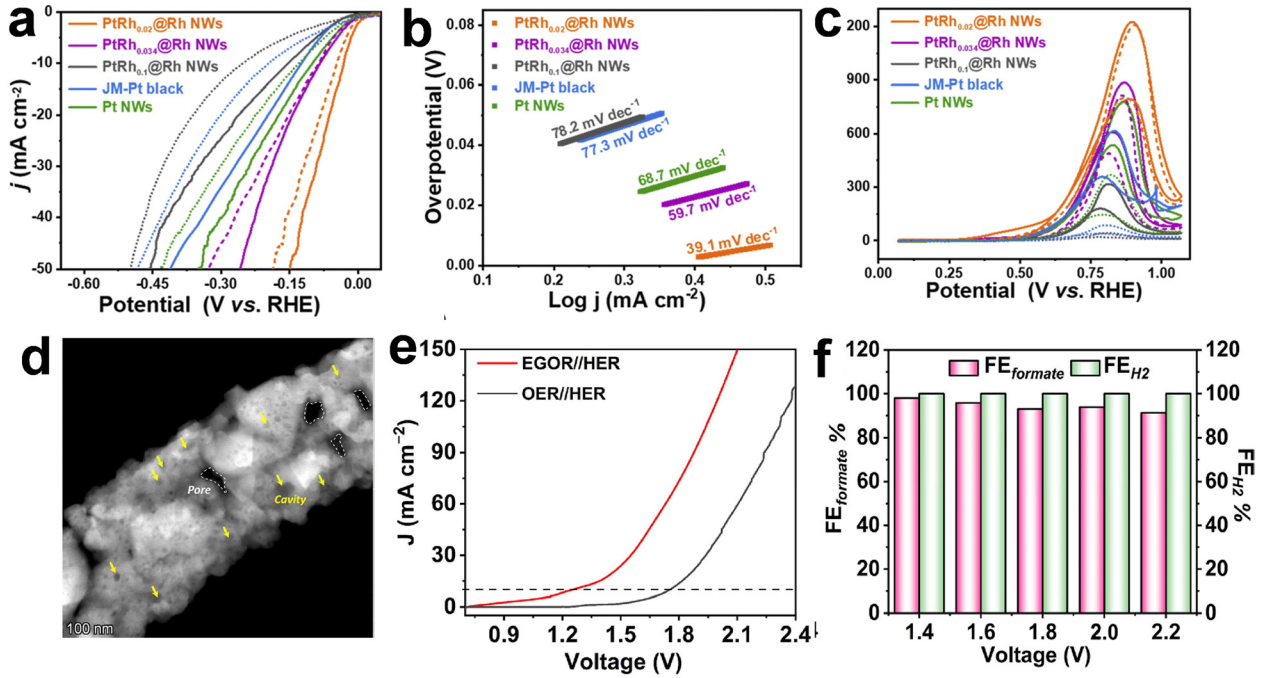

Fig. 14 $PtRh_{0.02}$@NWs (a) HER performance comparison diagram, (b) Tafel slope diagram, (c) CV curves of $PtRh_{0.02}$@Rh NW, $PtRh_{0.034}$@Rh NW, $PtRh_{0.1}$@Rh NW in 0.1 M KOH with 0.6 M EG, reproduced with permission.[10] Copyright 2022, Royal Society of Chemistry. (d) TEM image of h-Ru-Cu_xO, (e) LSV, (f) schematic diagram of Faraday efficiency of formate and H_2 production in HER//EGOR reaction system in a two-electrode system, reproduced with permission.[78] Copyright 2023, Elsevier.

electron migration, thus accelerating mass transfer and bubble release. Moreover, the rich cavity structure of the structure also further accelerated the transfer of electrons (Fig. 14e). The electrochemical test results showed that the h-Ru-Cu_xO/CF electrode materials were able to reach different current densities (10, 100, 200 mA cm^{-2}) at lower potentials, which further demonstrated the excellent catalytic activity of the catalysts. In the electrolysis system consisting of HER//EGOR, a current density of 10 mA cm^{-2} could be achieved with only 1.26 V, which is about 610 mV lower than that of the all-water reaction, confirming that the coupling of EGOR and HER can achieve efficient hydrogen production. Fig. 14f shows that the formate FE at the anode of the electrolysis cell exceeded 90%, and the FE at the cathode for the reaction with HER could reach nearly 100% H_2. In fact, the electrocatalytic oxidation of EG coupled with hydrogenation reaction already has a certain economic value. During the reaction process, it can produce a variety of high-value-added chemicals, such as formic acid and glycolic acid, to meet the needs of multiple fields, and it can also provide clean hydrogen for the hydrogen energy industry, creating considerable revenue. At the same time, it can reduce the energy consumption of hydrogen production by electrolysis of water and utilize cheap glycol raw materials, effectively saving costs. It can even convert the glycol in waste plastics and industrial wastewater into useful products and realize resource recycling.

4.3.2 EGOR coupled with other reactions. Recently, researchers have also chosen to couple EG oxidation and carbon dioxide reduction reactions,[79–81] such as the $Pd_{67}Ag_{33}$ electrocatalyst reported[82] just this year, due to the unique electronic structure of both EG oxidation and electrochemical CO_2 reduction reaction. This is because the transfer of neutrons of $Pd_{67}Ag_{33}$ from Ag to Pd results in an increase in the electron filling of the Pd d-band and a downward shift in the Pd D-band centre. This downward shift in the D-band centre weakens the binding strength on the catalyst and promotes the desorption of the carbonyl intermediates, which is critical for inhibiting C–C bond breakage and improving selectivity for C2 products. Meanwhile, aberration-corrected large-angle toroidal dark-field scanning HAADF-STEM images reveal a large number of amorphous regions, defects, and boundaries. In contrast, Pd shows regularly arranged lattice stripes, indicating the presence of lower defects that lead to changes in electron distribution that provide more reaction sites. The HRTEM diagram shows (Fig. 15a) that the lattice spacing of the (111) crystal faces of Pd is 2.244 Å, while the lattice spacing of $Pd_{67}Ag_{33}$ in the same region is 2.328 Å. This is due to lattice expansion of $Pd_{67}Ag_{33}$ resulting in lattice strain caused by Ag alloying into the Pd lattice (Fig. 15b). As shown in Fig. 15c, LSV results show that when EG is present in the electrolyte, the $Pd_{67}Ag_{33}$ catalytic electrode requires only 0.63 V voltage to reach 10 mA cm^{-2}. At the same time, the catalytic electrode also has a low Tafel slope during the reaction process, which is due to the precise regulation of the electron and lattice structure leading to its excellent oxidation kinetics. As shown in Fig. 15d, the excellent catalytic activity of the catalyst is further

 This journal is © The Royal Society of Chemistry 2025

Published on 12 d'abril 2025. Downloaded on 14/2/2026 0:11:27.

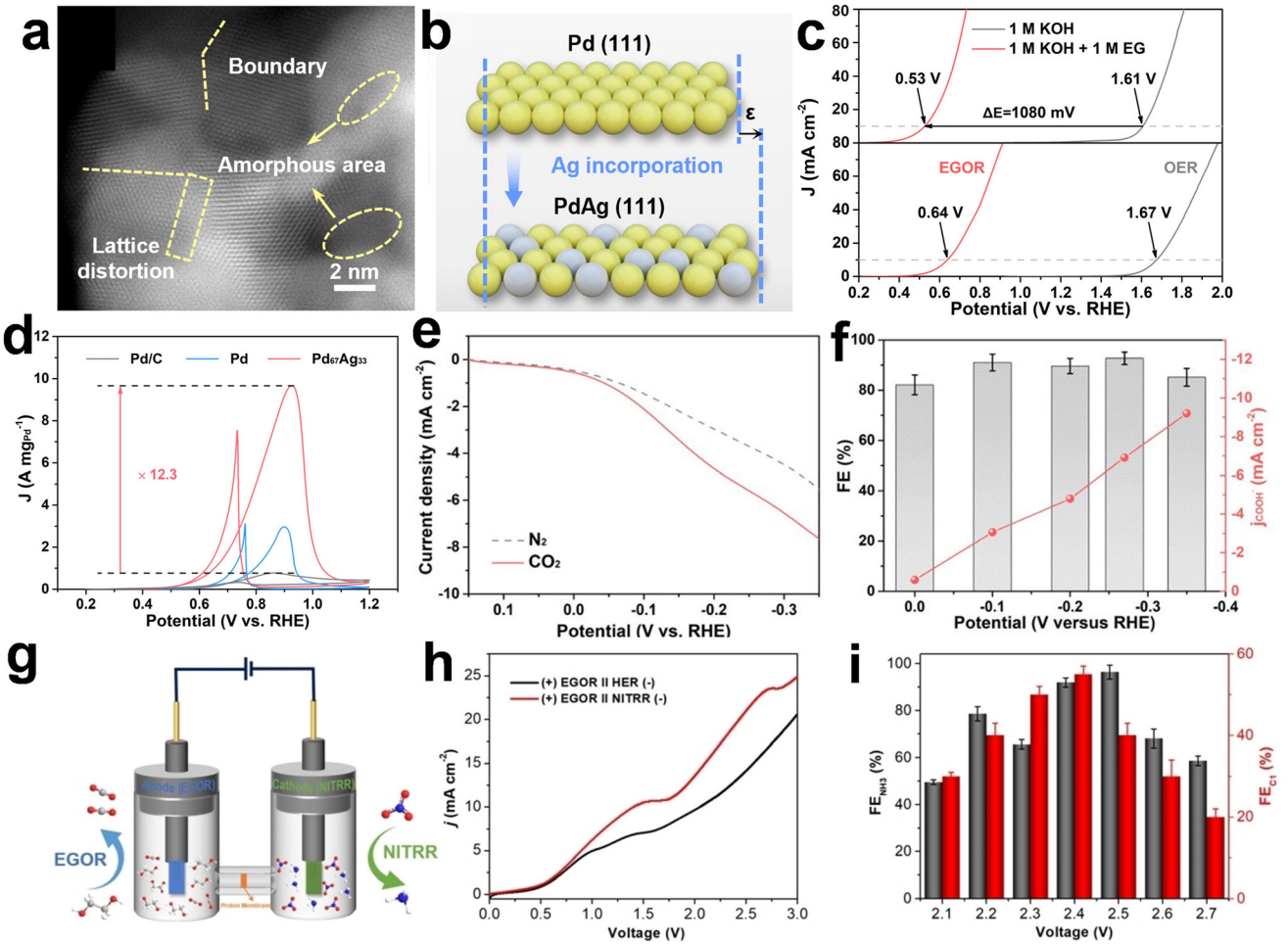

Fig. 15 (a)TEM diagram of $Pd_{67}Ag_{33}$, (b) lattice expansion diagram, (c) electrocatalytic performance diagram of anode EGOR, (d) CV diagram in 1 M KOH with 1 M EG, (e) CO_2RR performance diagram, (f) Faraday efficiency diagram of cathode CO_2RR reduction products, reproduced with permission.[82] Copyright 2024, National Academy of Sciences. EGOR//NITRR reaction system in a two-electrode system, (g) schematic diagram, (h) performance diagram, (i) schematic diagram of Faraday efficiency of product generation, reproduced with permission.[85] Copyright 2024, John Wiley and Sons.

confirmed, and the unique electronic structure of $Pd_{67}Ag_{33}$ inhibits the toxicity of CO, thereby facilitating the electrochemical CO_2, which provides a high current density of 10.8 mA cm^{-2} at −0.36 V (Fig. 15e). It also provides a maximum Faraday efficiency of 92.6% for FA production at −0.27 V. (Fig. 15f). In the whole reaction process, glycol can not only be obtained through various ways such as from petrochemicals and biomass conversion, but can also be extracted from waste plastics and other recyclables to achieve the recycling of resources, which greatly reduces the cost of raw material procurement. Carbon dioxide, as a major industrial waste gas, is relatively less difficult to collect and less costly, and its resourceful utilization through coupling reactions further reduces the enterprise's expenditure on raw materials. In terms of energy consumption, compared with the traditional electrolysis of water to produce hydrogen, carbon dioxide reduction and other separate high-energy chemical reactions, the coupling reaction cleverly exploits the synergy between the two reactions, optimizes the efficiency of energy use, reduces the overall cost of energy consumption, and makes the production process more economical and efficient, which improves the economic efficiency of the enterprise.

In addition to coupling with the carbon dioxide reduction reaction (CO_2RR), the EG oxidation reaction and nitrate reduction reaction can also be coupled.[82–84] Nitrate reduction reaction is a typical multi-electron reaction process. An urgent problem is the selection a suitable catalyst to achieve nitrate reduction. Lv *et al.*[85] reported Ir-doped CuPd (Ir-CuPd) single-crystal mesoporous nano-tetrahedra (SMTs) and further explored their use as highly active, stable, and selective electrocatalysts for alkaline EGOR electrocatalytic activity. At the same time, the catalyst showed good electrocatalytic performance in the coupled electrocatalysis of EGOR and nitrate reduction reaction (NITRR). The catalytic electrode had a stable structure and the elements were uniformly distributed in a concave tetragonal form. The size was between 63 and

Published on 12 d'abril 2025. Downloaded on 14/2/2026 0:11:27.

86 nm, and there were old pores in the interior. As shown in Fig. 15g, a dual-motor test system was constructed in the H-type battery for testing ((+) EGOR//NITRR (−)), where the anode was the EGOR and the NITRR was the cathode reaction. Compared with the traditional HER, the reaction system had a lower initial potential, indicating that the catalyst as a bifunctional catalyst has a high efficiency catalytic electrode. Fig. 15h shows that Ir-CuPd had higher electrocatalytic efficiency and lower energy consumption in the coupling system of glycol oxidation and nitrate reduction reactions. A higher selectivity of the catalyst was obtained in a two-electrode coupling system compared with a half-reaction (Fig. 15i). The dual-function Ir-CuPd SMT showed the highest Faraday efficiency of 66.2% at 2.4 V in anode EGOR electrocatalysis and 96.4% at 2.6 V in cathode NITRR electrocatalysis. This further proves that Ir-CuPd catalyst is an efficient bi-functional electrocatalytic catalyst. As one of the main pollutants of eutrophication in water bodies, the reduction of nitrate to harmless nitrogen or usable ammonia nitrogen has far-reaching significance for environmental protection. The nitrate reduction product, ammonia nitrogen, can be used as an important chemical raw material, which is widely used in many industries such as fertilizers and pharmaceuticals, and can be directly used in industrial production to reduce the cost of raw material procurement. The oxidation process of EG can also produce oxidation products with certain economic value, which realizes the efficient use and recycling of resources and reduces the dependence on primary resources.

5. Conclusion and outlook

Many studies have shown that transition metal catalysts have promising applications in the field of EG oxidation. Although catalysts based on transition metal noble metals are relatively rare,[41,86–90] it has been reported that loading a small amount of noble metal single atoms on non-precious metal catalysts can lead to high catalytic performance.[19,43,80,91] Therefore, the selection of suitable synthetic methods can often purposefully modulate the morphology, structure and size of the catalysts, and the use of more advanced characterisation tests can further reveal the micro-mechanisms of EG oxidation and the underlying reasons for the excellent performance, leading to the preparation of highly active catalysts. Despite the great progress in transition metal-catalysed EG oxidation, there are still some challenges to be solved.

The mechanism is not well understood: for the oxidation of EG, different oxidation pathways are caused by different intermediates during the reaction.[92–96] The ideal is to achieve complete oxidation through the C1 pathway,[35] releasing more electrons and achieving higher energy efficiency, ultimately resulting in valuable value-added products. However, due to the inappropriate adsorption energy of many transition metal electrocatalysts with intermediate products, the C–C bond-breaking ability is weak, and the reaction is mainly incomplete oxidation through the C2 pathway, in which it is difficult to achieve high energy conversion efficiency. *In situ* characterization techniques, such as *in situ* infrared spectroscopy and *in situ* X-ray absorption spectroscopy, have been used to monitor the changes in the structure and electronic state of the catalyst during the reaction process in real time, so as to deeply understand the catalytic reaction mechanism and the factors affecting the C–C bond fracture, providing a basis for the design and optimization of the catalyst.

Limited reaction sites of catalysts: currently prepared transition metal catalysts have limited ability to resist poisoning. In the oxidation reaction of EG, the intermediate products produced during the reaction may be adsorbed on the surface of the catalyst, leading to catalyst poisoning, reducing its catalytic activity. For example, CO, a common intermediate in glycol oxidation reactions, is easily adsorbed on the surface of the transition metal, occupying the active site and affecting the performance of the catalyst. When the active site of the transition metal electrocatalyst is partially covered or blocked, the utilization of the active site is not high, which affects the rate of the catalytic reaction. This requires the purposeful regulation of more exposed active sites during the synthesis process, such as the use of nanotechnology to prepare transition metal electrocatalysts with specific morphology and size, such as nanoparticles, nanowires, nanosheets, *etc*., which can increase the specific surface area and the number of active sites of the catalyst, and improve the catalytic performance.

Single regulation strategy: the current regulation strategy for transition metal catalysts mainly focuses on single-atom doping[97] and alloying. The single-atom catalyst has high atomic utilization and a unique electronic structure, which has great potential in the EG oxidation reaction. By precisely controlling the dispersion and coordination environment of transition metal atoms on the support, efficient monatomic catalysts can be prepared. For example, by loading precious metal single atoms on a non-precious metal catalyst, the precious metal is dispersed on the carrier in the form of single atoms, which can improve the atomic utilization and increase the number of active sites. However, the choice of carrier is particularly important. (1) Porous material carrier:[98–103] these carriers have a large surface area and rich pore structure, can provide more active sites, and help the diffusion of reactants and products. For example, the precious metal catalyst with alumina as the carrier has a good catalytic effect in the glycol oxidation reaction. (2) Two-dimensional material carriers: two-dimensional materials such as graphene, transition metal disulfide, *etc*., have also become ideal carriers for precious metal catalysts due to their unique electronic structure and physical properties. Two-dimensional materials can interact with precious metals, regulate the electronic structure of precious metals, and improve the activity and selectivity of catalysts. Although single-atom catalysts have been proved to have good application prospects, more catalysts are needed, such as through interface engineering to regulate the electronic structure of the catalyst to achieve high activity.[42,104–106]

Challenge of combined factors: the oxidation performance of EG is not only affected by the catalyst, but temperature and

 This journal is © The Royal Society of Chemistry 2025

Published on 12 d'abril 2025. Downloaded on 14/2/2026 0:11:27.

pressure are also important factors affecting the oxidation reaction of EG. Appropriately increasing the reaction temperature and pressure can improve the reaction rate, but too high a temperature and pressure may lead to catalyst deactivation or side reactions. Therefore, researchers need to optimise the reaction temperature and pressure to improve the efficiency and selectivity of EG oxidation; choosing the right concentration of reactants can also improve the reaction rate and yield, so many aspects need to be considered to achieve efficient EG oxidation. In addition, the study of transition metal catalysis for electrocatalytic EG oxidation has also had a positive impact on related fields, providing key technological support for the development of new types of fuel cells and electrolysers, which is expected to improve the efficiency of energy conversion, reduce energy consumption, and reduce environmental pollution.[107–110] This work further elaborates that the coupling of EG with other reactions, such as the carbon dioxide reduction reaction, not only achieves efficient oxidation of EG, but also solves the problem of energy pollution, which is of far-reaching significance for future sustainable development.

In conclusion, this work focuses on the summary of transition metal catalysts currently used for the electrocatalytic oxidation of EG. Firstly, the mechanism of electrocatalytic oxidation of EG is explained, and furthermore, different synthetic strategies currently used for the synthesis of the catalysts are summarized, providing a reference synthetic strategy for the design and preparation of subsequent catalysts for the electrocatalytic oxidation of EG. Subsequently, the common non-precious metal catalysts and precious metal catalysts are summarized and their excellent properties are explained. Finally, the opportunities and challenges for the future are explained, which will provide a reference for the future investigation of efficient catalysts for the electrocatalytic oxidation of EG and their effects on EGOR to effectively control the intermediate products of EG and ultimately produce the target oxidation products.

Author contributions

Hongjing Wu: conceptualization, formal analysis, investigation, visualization, writing – original draft. Xiaoyue Zheng, Jiajia Liu, and Yanru Yuan: investigation, visualization. Yuquan Yang, Chenjing Wang, Li Zhou, and Lulu Wang: investigation, formal analysis. Binbin Jia and Xiaoyu Fan: conceptualization, formal analysis, writing – review & editing. Jinlong Zheng: conceptualization, formal analysis, writing – review & editing, resources, supervision, funding acquisition.

Data availability

No primary research results, software or code have been included and no new data were generated or analyzed as part of this review.

Conflicts of interest

There is no conflict to declare.

Acknowledgements

This work was financially supported by the National Natural Science Foundation of China [52271200] and Guangdong Basic and Applied Basic Research Foundation [2024A1515010393]. Graphical abstract image contains material reproduced with permission from: [16]Copyright 2021, John Wiley and Sons, [44]Copyright 2023, John Wiley and Sons, [46]Copyright 2024, American Chemical Society, [49]Copyright 2024, John Wiley and Sons, [27]Copyright 2023, John Wiley and Sons and [1]Copyright 2022, American Chemical Society.

References

1 J. Wang, X. Li, M. Wang, *et al.*, Electrocatalytic Valorization of Poly (ethylene terephthalate) Plastic and CO_2 for Simultaneous Production of Formic Acid, *ACS Catal.*, 2022, **12**, 6722–6728.
2 V. Tournier, C. M. Topham, A. Gilles, *et al.*, An engineered PET depolymerase to break down and recycle plastic bottles, *Nature*, 2020, **580**, 216–219.
3 Y. Yan, H. Zhou, S.-M. Xu, *et al.*, Electrocatalytic Upcycling of Biomass and Plastic Wastes to Biodegradable Polymer Monomers and Hydrogen Fuel at High Current Densities, *J. Am. Chem. Soc.*, 2023, **145**, 6144–6155.
4 M. S. Kim, H. Chang, L. Zheng, *et al.*, A Review of Biodegradable Plastics: Chemistry, Applications, Properties, and Future Research Needs, *Chem. Rev.*, 2023, **123**, 9915–9939.
5 P. De Luna, C. Hahn, D. Higgins, *et al.*, What would it take for renewably powered electrosynthesis to displace petrochemical processes?, *Science*, 2019, **364**, eaav3506.
6 A. M. Hilbrands, M. K. Goetz and K.-S. Choi, C–C Bond Formation Coupled with C–C Bond Cleavage during Oxidative Upgrading of Glycerol on a Nanoporous $BiVO_4$ Photoanode, *J. Am. Chem. Soc.*, 2023, **145**, 25382–25391.
7 H. Zhou, Y. Ren, Z. Li, *et al.*, Electrocatalytic upcycling of polyethylene terephthalate to commodity chemicals and H_2 fuel, *Nat. Commun.*, 2021, **12**, 4679.
8 Q. Shi, W. Tang, K. Kong, *et al.*, Electrocatalytic Upgrading of Plastic and Biomass–Derived Polyols to Formamide under Ambient Conditions, *Angew. Chem., Int. Ed.*, 2024, **63**, e20240758.
9 A. K. Vijh, Anodic oxidation-of-ethylene-glycol-on-Pt-a-mechanistic-study, *Can. J. Chem.*, 1971, **49**, 94257271.
10 X. Jiang, Z. Dong, Q. Zhang, *et al.*, Decoupled hydrogen evolution from water/seawater splitting by integrating Ethylene Glycol oxidation on $PtRh_{0.02}$@Rh nanowires with Rh atom modification, *J. Mater. Chem. A*, 2022, **10**, 20571–20579.

Published on 12 d'abril 2025. Downloaded on 14/2/2026 0:11:27.

11 X. Wei, Z. Shen, R. Wei, *et al.*, Engineering p-d orbital hybridization in PdSb bimetallene for energy-saving H_2 production parallel upgrade plastic waste, *Chem. Eng. J.*, 2024, **498**, 155104.
12 Z. Li, Y. Yan, S.-M. Xu, *et al.*, Alcohols electrooxidation coupled with H_2 production at high current densities promoted by a cooperative catalyst, *Nat. Commun.*, 2022, **13**, 147.
13 L. Li, X. Cao, J. Huo, *et al.*, High valence metals engineering strategies of Fe/Co/Ni-based catalysts for boosted OER electrocatalysis, *J. Energy Chem.*, 2023, **76**, 195–213.
14 A. Muzammil, R. Haider, W. Wei, *et al.*, Emerging transition metal and carbon nanomaterial hybrids as electrocatalysts for water splitting: a brief review, *Mater. Horiz.*, 2023, **10**, 2764–2799.
15 H. Wang, B. Jiang, T.-T. Zhao, *et al.*, Electrocatalysis of Ethylene Glycol Oxidation on Bare and Bi-Modified Pd Concave Nanocubes in Alkaline Solution: An Interfacial Infrared Spectroscopic Investigation, *ACS Catal.*, 2017, **7**, 2033–2041.
16 B. Qiao, T. Yang, S. Shi, *et al.*, Highly Active Hollow RhCu Nanoboxes toward Ethylene Glycol Electrooxidation, *Small*, 2021, **17**, 2006534.
17 X. Yang, K. X. Yao, J. Y. Ye, *et al.*, Interface–Rich Three–Dimensional Au–Doped PtBi Intermetallics as Highly Effective Anode Catalysts for Application in Alkaline Ethylene Glycol Fuel Cells, *Adv. Funct. Mater.*, 2021, **31**, 2103671.
18 J. Qi, Z. An, C. Li, *et al.*, Electrocatalytic selective oxidation of Ethylene Glycol: A concise review of catalyst development and reaction mechanism with comparison to thermocatalytic oxidation process, *Curr. Opin. Electrochem.*, 2022, **32**, 100929.
19 Y. Qin, W. Zhang, F. Wang, *et al.*, Extraordinary p–d Hybridization Interaction in Heterostructural Pd–PdSe Nanosheets Boosts C–C Bond Cleavage of Ethylene Glycol Electrooxidation, *Angew. Chem., Int. Ed.*, 2022, **61**, e202200899.
20 Y. Zhang, D. Zhang, Y. Qin, *et al.*, Ultra-fast phosphating synthesis of metastable crystalline phase-controllable ultra-small MP_x/CNT (M=Pd, Pt, Ru) for polyalcohol electrooxidation, *J. Energy Chem.*, 2022, **72**, 108–115.
21 W. Yang, X. Yang, J. Jia, *et al.*, Oxygen vacancies confined in ultrathin Nickel oxide nanosheets for enhanced electrocatalytic methanol oxidation, *Appl. Catal., B*, 2019, **244**, 1096–1102.
22 Y. Li, F. Li, Y. Zhao, *et al.*, Iron doped cobalt phosphide ultrathin nanosheets on Nickel foam for overall water splitting, *J. Mater. Chem. A*, 2019, **7**, 20658–20666.
23 T.-J. Wang, G.-R. Xu, H.-Y. Sun, *et al.*, Anodic hydrazine electrooxidation boosted overall water electrolysis by bifunctional porous Nickel phosphide nanotubes on Ni foam, *Nanoscale*, 2020, **12**, 11526–11535.
24 F. Zhao, Q. Yuan, S. Nie, *et al.*, Modified electronic structure and enhanced hydroxyl adsorption make quaternary Pt-based nanosheets efficient anode electrocatalysts for formic acid-/alcohol-air fuel cells, *J. Energy Chem.*, 2024, **92**, 142–150.
25 H. Lv, F. Lv, H. Qin, *et al.*, Single-Crystalline Mesoporous platinum and platinum - Copper Nanocubes for Highly Efficient Electrochemical CO_2. Reduction, *CCS Chem.*, 2022, **4**, 1376–1385.
26 K. Liu, P. Cao, W. Chen, *et al.*, Electrocatalysis enabled transformation of earth-abundant water, nitrogen and carbon dioxide for a sustainable future, *Mater. Adv.*, 2022, **3**, 1359–1400.
27 G. Zhang, X. Li, K. Chen, *et al.*, Tandem Electrocatalytic Nitrate Reduction to Ammonia on MBenes, *Angew. Chem., Int. Ed.*, 2023, **62**, e202300054.
28 N. L. Chauhan, V. A. Juvekar and A. Sarkar, Oxidation of Ethylene Glycol: Unity of chemical and electrochemical catalysis, *Electrochem. Sci. Adv.*, 2021, **2**, e2100092.
29 N. L. Chauhan, V. Dameera, A. Chowdhury, *et al.*, Electrochemical oxidation of Ethylene Glycol in a channel flow reactor, *Catal. Today*, 2018, **309**, 126–132.
30 D. Fan, K. Guo, Q. Hao, *et al.*, Ultrathin RhCuAgPd/Pd nanowire heterostructures for Ethylene Glycol electrooxidation, *Chem. Commun.*, 2022, **58**, 7773–7776.
31 D. Fan, H. Yao, L. Sun, *et al.*, 2D PtRhPb Mesoporous Nanosheets with Surface–Clean Active Sites for Complete Ethanol Oxidation Electrocatalysis, *Adv. Mater.*, 2024, **36**, 2407940.
32 H. Lv, X. Guo, L. Sun, *et al.*, A universal strategy for fast, scalable, and aqueous synthesis of multicomponent palladium alloy ultrathin nanowires, *Sci. China: Chem.*, 2021, **64**, 245–252.
33 Q. Qian, X. He, Z. Li, *et al.*, Electrochemical Biomass Upgrading Coupled with Hydrogen Production under Industrial-Level Current Density, *Adv. Mater.*, 2023, **35**, 2300935.
34 Y. Wang, H. Lv, L. Sun, *et al.*, Ultrathin and Wavy PdB Alloy Nanowires with Controlled Surface Defects for Enhanced Ethanol Oxidation Electrocatalysis, *ACS Appl. Mater. Interfaces*, 2021, **13**, 17599–17607.
35 L. Sun, H. Lv, J. Xiao, *et al.*, Enzymatic Mesoporous Metal Nanocavities for Concurrent Electrocatalysis of Nitrate to Ammonia Coupled with Polyethylene Terephthalate Upcycling, *Adv. Mater.*, 2024, **36**, 2402767.
36 X.-Y. Ma, H.-Z. Ma, S.-H. He, *et al.*, The electrocatalytic activity and selectivity of EG oxidation into value-added chemicals at iron-group electrodes in alkaline media, *Mater. Today Phys.*, 2023, **37**, 101191.
37 A. Rabis, P. Rodriguez and T. J. Schmidt, Electrocatalysis for Polymer Electrolyte Fuel Cells: Recent Achievements and Future Challenges, *ACS Catal.*, 2012, **2**, 864–890.
38 X. Feng, L. Yang and L. Zhang, Sustainable solar-and electro-driven production of high concentration H_2O_2 coupled to electrocatalytic upcycling of polyethylene terephthalate plastic waste, *Chem. Eng. J.*, 2024, **482**, 149191.
39 G. Lin, H. Li and K. Xie, Twisted Surfaces in Porous Single Crystals to Deliver Enhanced Catalytic Activity and Stability, *Angew. Chem., Int. Ed.*, 2020, **59**, 16440–16444.

 This journal is © The Royal Society of Chemistry 2025

Published on 12 d'abril 2025. Downloaded on 14/2/2026 0:11:27.

40 Z. Guo, M. Liu, L. Ga, *et al.*, Terbium-doped cobalt-based metal–organic frameworks for electrocatalytic hydrogen production and polyethylene terephthalate plastic upcycling, *Chem. Eng. J.*, 2024, **496**, 154062.
41 M. You, X. Du, X. Hou, *et al.*, *In situ* growth of ruthenium-based nanostructure on carbon cloth for superior electrocatalytic activity towards HER and OER, *Appl. Catal., B*, 2022, **317**, 121729.
42 L. Jiao, W. Wei, X. Li, *et al.*, Value-added formate production from selective Ethylene Glycol oxidation based on cost-effective self-supported MOF nanosheet arrays, *Rare Met.*, 2022, **41**, 3654–3661.
43 K. Zhang, C. Wang, H. You, *et al.*, Advanced Plasmon-driven Ethylene Glycol oxidation over 3D ultrathin Lotus-like PdCu nanosheets, *Chem. Eng. J.*, 2022, **438**, 135666.
44 Y. Wang, J. Liu, H. Yuan, *et al.*, Strong Electronic Interaction between Amorphous MnO_2 Nanosheets and Ultrafine Pd Nanoparticles toward Enhanced Oxygen Reduction and Ethylene Glycol Oxidation Reactions, *Adv. Funct. Mater.*, 2023, **33**, 2211909.
45 J. Li, L. Li, X. Ma, *et al.*, Selective Ethylene Glycol Oxidation to Formate on Ni Selenide with Simultaneous Evolution of Hydrogen, *Adv. Sci.*, 2023, **10**, 2300841.
46 H. Kang, D. He, X. Yan, *et al.*, Cu Promoted the Dynamic Evolution of Ni-Based Catalysts for Polyethylene Terephthalate Plastic Upcycling, *ACS Catal.*, 2024, **14**, 5314–5325.
47 R.-C. Li, X.-Y. Zhang, Z.-Y. Qu, *et al.*, One-step controlled electrodeposition Ni sulfides heterointerfaces favoring the desorption of hydroxyl groups for efficient hydrogen generation, *Rare Met.*, 2024, **43**, 4377–4386.
48 N. Wang, X. Li, M.-K. Hu, *et al.*, Ordered macroporous superstructure of bifunctional cobalt phosphide with heteroatomic modification for paired hydrogen production and polyethylene terephthalate plastic recycling, *Appl. Catal., B*, 2022, **316**, 121667.
49 J. Zhang, X. Zhang, C. Shi, *et al.*, Plasma–Constructed Co_2P–Ni_2P Heterointerface for Electro-Upcycling of Polyethylene Terephthalate Plastic to Co–Produce Hydrogen and Formate, *Small*, 2024, **20**, 2406767.
50 T. Wan, X. Huang, S. Li, *et al.*, Fabrication of 3D hollow acorn-shell-like PtBi intermetallics via a surfactant-free pathway for efficient Ethylene Glycol electrooxidation, *Nano Res.*, 2023, **16**, 6560–6567.
51 F. Kong, X. Liu, Y. Song, *et al.*, Selectively Coupling Ru Single Atoms to PtNi Concavities for High–Performance Methanol Oxidation via d–Band Center Regulation, *Angew. Chem., Int. Ed.*, 2022, **61**, e202207524.
52 Y. Zhang, X. Liu, T. Liu, *et al.*, Rhombohedral Pd–Sb Nanoplates with Pd–Terminated Surface: An Efficient Bifunctional Fuel–Cell Catalyst, *Adv. Mater.*, 2022, **34**, 2202333.
53 Q. Shang, N. Tang, H. Qi, *et al.*, A platinum single-atom catalyst toward efficient activation of molecular oxygen for cinnamyl alcohol oxidation, *Chin. J. Catal.*, 2020, **41**, 1812–1817.
54 X. Liu, Z. Fang, D. Xiong, *et al.*, Upcycling PET in parallel with energy-saving H_2 production via bifunctional Ni-cobalt nitride nanosheets, *Nano Res.*, 2022, **16**, 4625–4633.
55 K. Liu, Y. Wang, F. Liu, *et al.*, Selective electrocatalytic reforming of PET-derived Ethylene Glycol to formate with a Faraday efficiency of 93.2% at industrial-level current densities, *Chem. Eng. J.*, 2023, **473**, 145292.
56 Y. Lin, Y. Chen, H. Ren, *et al.*, Inspiration of Bimetallic Peroxide for Controllable Electrooxidizing Ethylene Glycol Through Modulating Surficial Intermediates, *Adv. Funct. Mater.*, 2024, **34**, 2404594.
57 J. Zheng, X. Peng, Z. Xu, *et al.*, Cationic Defect Engineering in Spinel $NiCo_2O_4$ for Enhanced Electrocatalytic Oxygen Evolution, *ACS Catal.*, 2022, **12**, 10245–10254.
58 Q. Sun, Y.-Y. Zheng, L.-X. Yun, *et al.*, Fe_3O_4 Nanodispersions as Efficient and Recoverable Magnetic Nanocatalysts for Sustainable PET Glycolysis, *ACS Sustainable Chem. Eng.*, 2023, **11**, 7586–7595.
59 H. Zhang, Z. Liu, H. Li, *et al.*, PdFe alloy nanoparticles supported on nitrogen-doped carbon nanotubes for electrocatalytic upcycling of poly (ethylene terephthalate) plastics into formate coupled with hydrogen evolution, *J. Mater. Chem. A*, 2024, **12**, 15984–15995.
60 H. Lei, N. Ma, K. Li, *et al.*, Low Pt loading with lattice strain for direct Ethylene Glycol fuel cells, *Energy Environ. Sci.*, 2024, **17**, 7792–7802.
61 J. Wang, X. Li, T. Zhang, *et al.*, Electro-Reforming Polyethylene Terephthalate Plastic to Co-Produce Valued Chemicals and Green Hydrogen, *J. Phys. Chem. Lett.*, 2022, **13**, 622–627.
62 F. Gao, Y. Zhang, H. You, *et al.*, Solvent–Mediated Shell Dimension Reconstruction of Core@Shell PdAu@Pd Nanocrystals for Robust C1 and C2 Alcohol Electrocatalysis, *Small*, 2021, **17**, 2101428.
63 C. Jin, C. Sun, R. Dong, *et al.*, Pt modification of gold and electrocatalytic oxidation of Ethylene Glycol on Pt-modified Au electrodes, *Electrochim. Acta*, 2010, **56**, 321–325.
64 H. Pu, K. Dong, T. Zhang, *et al.*, Regulation of the shell thickness and shell components in PtCu/PdCu core–shell tripods for Ethylene Glycol and glycerol oxidation reactions, *J. Mater. Chem. A*, 2022, **10**, 10614–10624.
65 M. Song, Y. Wu, Z. Zhao, *et al.*, Corrosion Engineering of Part–Per–Million Single Atom Pt/$Ni(OH)_2$ Electrocatalyst for PET Upcycling at Ampere–Level Current Density, *Adv. Mater.*, 2024, **36**, 2403234.
66 O. Ambriz-Peláez, S. Durón, A. Olivas, *et al.*, Effect of molybdenum content on the morphology and electronic characteristics of Pd–MoO_x nanomaterials and activity evaluation for EG electro–oxidation, *Appl. Surf. Sci.*, 2019, **498**, 143842.
67 Q. Mao, K. Deng, H. Yu, *et al.*, In Situ Reconstruction of Partially Hydroxylated Porous Rh Metallene for EG–Assisted Seawater Splitting, *Adv. Funct. Mater.*, 2022, **32**, 2201081.
68 G. Ma, N. Yang, Y. Xue, *et al.*, Ethylene Glycol Electrochemical Reforming Using Ruthenium

Published on 12 d'abril 2025. Downloaded on 14/2/2026 0:11:27.

Nanoparticle-Decorated Ni Phosphide Ultrathin Nanosheets, *ACS Appl. Mater. Interfaces*, 2021, **13**, 42763–42772.

69 Y. Li, X. Liu, K. Wang, *et al.*, Oxygen vacancy assisted Ru–$Ni(OH)_2$ for efficient ethylene glycol electrooxidation reaction, *Inorg. Chem. Front.*, 2024, **11**, 6889–6897.

70 X. Liu, Y. Han, Y. Guo, *et al.*, Electrochemical Hydrogen Generation by Oxygen Evolution Reaction–Alternative Anodic Oxidation Reactions, *Adv. Energy Sustainability Res.*, 2022, **3**, 2200005.

71 F. Arshad, T. U. Haq, I. Hussain, *et al.*, Recent Advances in Electrocatalysts toward Alcohol-Assisted, Energy-Saving Hydrogen Production, *ACS Appl. Energy Mater.*, 2021, **4**, 8685–8701.

72 L. Fan, Y. Ji, G. Wang, *et al.*, High Entropy Alloy Electrocatalytic Electrode toward Alkaline Glycerol Valorization Coupling with Acidic Hydrogen Production, *J. Am. Chem. Soc.*, 2022, **144**, 7224–7235.

73 B. Mondal, N. Karjule, C. Singh, *et al.*, Unraveling the Mechanisms of Electrocatalytic Oxygenation and Dehydrogenation of Organic Molecules to Value–Added Chemicals Over a Ni–Fe Oxide Catalyst, *Adv. Energy Mater.*, 2021, **11**, 2101858.

74 L. Wang, Y. Zhu, Y. Wen, *et al.*, Regulating the Local Charge Distribution of Ni Active Sites for the Urea Oxidation Reaction, *Angew. Chem., Int. Ed.*, 2021, **60**, 10577–10582.

75 T. Wang, X. Cao, L. Jiao, *et al.*, Progress in Hydrogen Production Coupled with Electrochemical Oxidation of Small Molecules, *Angew. Chem., Int. Ed.*, 2022, **61**, e202213328.

76 Y. Xu and B. Zhang, Recent Advances in Electrochemical Hydrogen Production from Water Assisted by Alternative Oxidation Reactions, *ChemElectroChem*, 2019, **6**, 3214–3226.

77 Z. Wang, J. Li, Q. Zhang, *et al.*, Facilitating Formate Selectivity via Optimizing eg* Band Broadening in NiMn Hydroxides for Ethylene Glycol Electro–Oxidation, *Angew. Chem., Int. Ed.*, 2024, **63**, e202411517.

78 L. Liu, Y. He, D.-D. Ma, *et al.*, Directional editing of self-supported nanoarray electrode for adaptive paired-electrolysis, *J. Colloid Interface Sci.*, 2023, **640**, 423–433.

79 G. Wang, J. Chen, Y. Ding, *et al.*, Electrocatalysis for CO_2 conversion: from fundamentals to value-added products, *Chem. Soc. Rev.*, 2021, **50**, 4993–5061.

80 C. Tang, Y. Zheng, M. Jaroniec, *et al.*, Electrocatalytic Refinery for Sustainable Production of Fuels and Chemicals, *Angew. Chem., Int. Ed.*, 2021, **60**, 19572–19590.

81 P. Zhu and H. Wang, High-purity and high-concentration liquid fuels through CO_2 electroreduction, *Nat. Catal.*, 2021, **4**, 943–951.

82 C. Junliang, Z. Fangzhou, K. Min, *et al.*, Unveiling synergy of strain and ligand effects in metallic aerogel for electrocatalytic polyethylene terephthalate upcycling proceedings of the National Academy of Sciences, *Proc. Natl. Acad. Sci. U. S. A.*, 2024, **121**, e2318853121.

83 L. Xiao, W. Dai, S. Mou, *et al.*, Coupling electrocatalytic cathodic nitrate reduction with anodic formaldehyde oxidation at ultra-low potential over Cu_2O, *Energy Environ. Sci.*, 2023, **16**, 2696–2704.

84 S. Han, H. Li, T. Li, *et al.*, Ultralow overpotential nitrate reduction to ammonia via a three-step relay mechanism, *Nat. Catal.*, 2023, **6**, 402–414.

85 H. Lv, Y. Mao, H. Yao, *et al.*, Ir–Doped CuPd Single–Crystalline Mesoporous Nanotetrahedrons for Ethylene Glycol Oxidation Electrocatalysis: Enhanced Selective Cleavage of C–C Bond, *Angew. Chem., Int. Ed.*, 2024, **63**, e202400281.

86 S.-Y. Bae, J. Mahmood, I.-Y. Jeon, *et al.*, Recent advances in ruthenium-based electrocatalysts for the hydrogen evolution reaction, *Nanoscale Horiz.*, 2020, **5**, 43–56.

87 B. Geng, F. Yan, X. Zhang, *et al.*, Conductive CuCo–Based Bimetal Organic Framework for Efficient Hydrogen Evolution, *Adv. Mater.*, 2021, **33**, 2106781.

88 C.-B. Hong, X. Li, W.-B. Wei, *et al.*, Nano-engineering of Ru-based hierarchical porous nanoreactors for highly efficient pH-universal overall water splitting, *Appl. Catal., B*, 2021, **294**, 120230.

89 Q. Tan, R. Xiao, X. Yao, *et al.*, Non-oxygen anion-regulated in situ cobalt based heterojunctions for active alkaline hydrogen evolution catalysis, *Chem. Eng. J.*, 2022, **433**, 133514.

90 F. Lv, W. Zhang, M. Sun, *et al.*, Au Clusters on Pd Nanosheets Selectively Switch the Pathway of Ethanol Electrooxidation: Amorphous/Crystalline Interface Matters, *Adv. Energy Mater.*, 2021, **11**, 2100187.

91 F. Gao, Y. Zhang, F. Ren, *et al.*, Universal Surfactant–Free Strategy for Self–Standing 3D Tremella–Like Pd-M (M = Ag, Pd, and Au) Nanosheets for Superior Alcohols Electrocatalysis, *Adv. Funct. Mater.*, 2020, **30**, 2000255.

92 T.-T. Zhuang, Y. Pang, Z.-Q. Liang, *et al.*, copper nanocavities confine intermediates for efficient electrosynthesis of C3 alcohol fuels from carbon monoxide, *Nat. Catal.*, 2018, **1**, 946–951.

93 H. Lv, L. Sun, Y. Wang, *et al.*, Highly Curved, Quasi–Single–Crystalline Mesoporous Metal Nanoplates Promote C-C Bond Cleavage in Ethanol Oxidation Electrocatalysis, *Adv. Mater.*, 2022, **34**, 2203612.

94 Y. Yoon, A. S. Hall, Y. Surendranath, *et al.*, Tuning of Silver Catalyst Mesostructure Promotes Selective Carbon Dioxide Conversion into Fuels, *Angew. Chem., Int. Ed.*, 2016, **55**, 15282–15286.

95 T. T. H. Hoang, S. Verma, S. Ma, *et al.*, Nanoporous copper–Silver Alloys by Additive-Controlled Electrodeposition for the Selective Electroreduction of CO_2 to Ethylene and Ethanol, *J. Am. Chem. Soc.*, 2018, **140**, 5791–5797.

96 Q. Lu, J. Rosen, Y. Zhou, *et al.*, A selective and efficient electrocatalyst for carbon dioxide reduction, *Nat. Commun.*, 2014, **5**, 3242.

97 H. Yu, T. Zhou, Z. Wang, *et al.*, Defect-Rich Porous platinum Metallene for Enhanced Alkaline Oxygen Reduction

 This journal is © The Royal Society of Chemistry 2025

Electrocatalysis, *Angew. Chem., Int. Ed.*, 2021, **60**, 12027–12031.
98 Z. W. Seh, J. Kibsgaard, C. F. Dickens, *et al.*, Combining theory and experiment in electrocatalysis: Insights into materials design, *Science*, 2017, **355**, eaad4998.
99 W. Wang, F. Lv, B. Lei, *et al.*, Tuning Nanowires and Nanotubes for Efficient Fuel–Cell Electrocatalysis, *Adv. Mater.*, 2016, **28**, 10117–10141.
100 M. A. Z. G. Sial, M. A. U. Din and X. Wang, Multimetallic nanosheets: synthesis and applications in fuel cells, *Chem. Soc. Rev.*, 2018, **47**, 6175–6200.
101 M. Iqbal, Y. V. Kaneti, J. Kim, *et al.*, Chemical Design of platinum-Based Nanoarchitectures for Catalytic Applications, *Small*, 2019, **15**, 1804378.
102 P. Prabhu and J.-M. Lee, Metallenes as functional materials in electrocatalysis, *Chem. Soc. Rev.*, 2021, **50**, 6700–6719.
103 L. Sun, H. Lv, J. Feng, *et al.*, Noble-Metal-Based Hollow Mesoporous Nanoparticles: Synthesis Strategies and Applications, *Adv. Mater.*, 2022, **34**, 2201954.
104 L. Zhang, S. Yu, J. Zhang, *et al.*, Porous single-crystalline AuPt@Pt bimetallic nanocrystals with high mass electrocatalytic activities, *Chem. Sci.*, 2016, **7**, 3500–3505.
105 L. Ye, S. Xi, H. Li, *et al.*, Surface Engineering in Mesoporous Single Crystal to Enhance Pseudocapacitance, *Adv. Funct. Mater.*, 2020, **31**, 374–384.
106 W. Li and K. Xie, Porous Single Crystals at the Macroscale: From Growth to Application, *Acc. Chem. Res.*, 2023, **56**, 374–384.
107 M. G. Kibria, J. P. Edwards, C. M. Gabardo, *et al.*, Electrochemical CO_2 Reduction into Chemical Feedstocks: From Mechanistic Electrocatalysis Models to System Design, *Adv. Mater.*, 2019, **31**, 1807166.
108 Y. Li, M. Wang, X. Liu, *et al.*, Catalytic Transformation of PET and CO_2 into High–Value Chemicals, *Angew. Chem., Int. Ed.*, 2022, **61**, e202117205.
109 S. Bhattacharjee, V. Andrei, C. Pornrungroj, *et al.*, Reforming of Soluble Biomass and Plastic Derived Waste Using a Bias–Free $Cu_{30}Pd_{70}$ Perovskite Pt Photoelectrochemical Device, *Adv. Funct. Mater.*, 2021, **32**, 2109313.
110 Y. Li, Y. Sun, Y. Qin, *et al.*, Recent Advances on Water–Splitting Electrocatalysis Mediated by Noble–Metal–Based Nanostructured Materials, *Adv. Energy Mater.*, 2020, **10**, 1903120.

Published on 12 d'abril 2025. Downloaded on 14/2/2026 0:11:27.